0013-7227/04/$15.00/0
Printed in U.S.A.

Endocrinology 145(2):951–958

doi: 10.1210/en.2003-0816

Androgen Contributes to Gender-Related Cardiac Hypertrophy and Fibrosis in Mice Lacking the Gene Encoding Guanylyl Cyclase-A

YUHAO LI, ICHIRO KISHIMOTO, YOSHIHIKO SAITO, MASAKI HARADA, KOICHIRO KUWAHARA, TAKEHIKO IZUMI, ICHIRO HAMANAKA, NOBUKI TAKAHASHI, RIKA KAWAKAMI, KEIJI TANIMOTO, YASUAKI NAKAGAWA, MICHIO NAKANISHI, YUICHIRO ADACHI, DAVID L. GARBERS, AKIYOSHI FUKAMIZU, AND KAZUWA NAKAO

Department of Medicine and Clinical Science (Y.L., I.K., Y.S., M.H., K.K., T.I., I.H., N.T., R.K., K.T., Y.N., M.N., Y.A., K.N.), Kyoto University Graduate School of Medicine, Kyoto 606-8501, Japan; Howard Hughes Medical Institute and Department of Pharmacology (D.L.G.), University of Texas, Southwestern Medical Center at Dallas, Dallas, Texas 75390; and Center for Tsukuba Advanced Research Alliance (A.F.), Institute of Applied Biochemistry, University of Tsukuba, Tsukuba, Ibaraki 305-8571, Japan

Myocardial hypertrophy and extended cardiac fibrosis are independent risk factors for congestive heart failure and sudden cardiac death. Before age 50, men are at greater risk for cardiovascular disease than age-matched women. In the current studies, we found that cardiac hypertrophy and fibrosis were significantly more pronounced in males compared with females of guanylyl cyclase-A knockout (GC-A KO) mice at 16 wk of age. These gender-related differences were not seen in wild-type mice. In the further studies, either castration (at 10 wk of age) or flutamide, an androgen receptor antagonist, markedly attenuated cardiac hypertrophy and fibrosis in male GC-A KO mice without blood pressure change. In contrast, ovariectomy (at 10 wk of age) had little effect. Also, chronic testosterone infusion increased cardiac mass and fibrosis in ovariectomized GC-A mice. None of the treatments affected cardiac mass or the extent of fibrosis in wild-type mice. Overexpression of mRNAs encoding atrial natriuretic peptide, brain natriuretic peptide, collagens I and III, TGF-β1, TGF-β3, angiotensinogen, and angiotensin converting enzyme in the ventricles of male GC-A KO mice was substantially decreased by castration. The gender differences were virtually abolished by targeted deletion of the angiotensin II type 1A receptor gene (AT1A). Neither castration nor testosterone administration induced any change in the cardiac phenotypes of double-KO mice for GC-A and AT1A. Thus, we suggest that androgens contribute to gender-related differences in cardiac hypertrophy and fibrosis by a mechanism involving AT1A receptors and GC-A. (*Endocrinology* 145: 951–958, 2004)

MYOCARDIAL HYPERTROPHY IS prevalent in a substantial portion of individuals with essential hypertension (1, 2), and it is recognized as an independent risk factor for congestive heart failure and sudden cardiac death (3). Extended cardiac fibrosis results in increased myocardial stiffness, causing ventricular dysfunction and, ultimately, heart failure (4). Significant gender-related differences in the cardiovascular system are now well documented, and before the age of 50, men are at greater risk for cardiovascular diseases than age-matched women (5–9). However, the precise mechanism underlying gender-related differences in cardiac diseases is not fully understood. The results of both *in vitro* and *in vivo* studies indicate that sex steroids play a key role in the development of cardiac structural abnormalities. Estrogen and androgen receptors are present in myocardial tissues (10–12). Estradiol has antiproliferative effects on cardiac fibroblasts (13) and vascular smooth-muscle cells (14, 15), whereas androgens increase proliferation of vascular smooth-muscle cells (16). Studies using sinoaortic denervation-induced cardiac hypertrophy in rats have also shown that testosterone facilitates hypertrophy but estradiol inhibits it (17). A less severe model of cardiac hypertrophy in rats (swimming- or hypertension-induced) failed to confirm the antiproliferative effect of estradiol (18). Moreover, not all males, whether human or experimental animal, develop gender-related cardiac abnormalities. Somjen and colleagues (15) reported a biphasic proliferative response for both estrogen and testosterone in vascular smooth muscle and endothelial cells. It, therefore, is unclear how gender-induced changes in cardiac structural pathology are made manifest.

Mice lacking guanylyl cyclase A (GC-A), a natriuretic peptide receptor, exhibit salt-resistant hypertension, myocardial hypertrophy and interstitial fibrosis, and sudden death (before the age of 6 months) (19–20). In the present study, we found that male GC-A knockout (KO) mice show more pronounced cardiac hypertrophy and fibrosis compared with female GC-A KO mice and that gender-related differences are not seen in wild-type (WT) mice. Additionally, we found that these gender-related differences are attenuated either by castration or flutamide, an androgen receptor (AR) antagonist, and abolished by genetic disruption of angiotensin

Abbreviations: ACE, Angiotensin converting enzyme; Agt, angiotensinogen; Ang, angiotensin; ANP, atrial natriuretic peptide; AR, androgen receptor; AT1A, Ang II type 1A; BNP, brain natriuretic peptide; BW, body weight; GC-A, guanylyl cyclase-A; HR, heart rate; KO, knockout; LVW, left ventricular weight; OVX, ovariectomy; SBP, systolic blood pressure; WT, wild-type.

Endocrinology is published monthly by The Endocrine Society (http://www.endo-society.org), the foremost professional society serving the endocrine community.

(Ang) II type 1A (AT1A) receptors in male GC-A KO mice. We propose that androgens contribute to gender-related differences in cardiac structure and that the AT1A receptor and GC-A are involved in a reciprocal fashion.

Materials and Methods

Animals and treatments

All experimental procedures were carried out in accordance with Kyoto University standards for animal care. GC-A KO mice were originally generated at the University of Texas, Southwestern Medical Center at Dallas and Howard Hughes Medical Institute. Mice were housed in groups of three to five per cage under climate-controlled conditions with a 12-h light/dark cycle and were provided with standard food (CRF-1; Oriental Yeast Co., Ltd, Tokyo, Japan) and water *ad libitum*. The WT (GC-A+/+, AT1A+/+), AT1A KO (GC-A+/+, AT1A−/−), GC-A KO (GC-A−/−, AT1A+/+), and double-KO (GC-A−/−, AT1A−/−) mice used in these experiments were generated from heterozygous (GC-A+/−, AT1A +/−) mice after crossing of single GC-A KO (19) and AT1A KO (21) mice. The genetic background of the original GC-A KO and AT1A KO mice was C57BL/6. Genotypes were determined before and verified after experimentation using PCR. Comparisons of age and body weight (BW) between the KO and WT mice were made among littermates. Also comparisons of age, body weight, and systolic blood pressure (SBP) between control and treated mice were performed.

Measurement of heart rate (HR) and SBP

HR and SBP were measured in conscious mice using a computerized tail-cuff method (Softron Co., Ltd., Tokyo, Japan) (19, 21). Briefly, mice were restrained in a pocket and warmed at 38 C. HR and SBP were measured at 1000–1400 h and calculated as the average of six sessions per day after mice were adapted to the apparatus for 5 d. The validity of this system has been established previously in our laboratory (22).

Measurement of left ventricular weight (LVW) and interstitial fibrosis

After animals were killed by cervical dislocation under anesthesia with ether at 16 wk of age, the hearts were dissected out, LVW was measured, and its ratio to BW (LVW/BW) was calculated and used as an index of ventricular hypertrophy. The left ventricles were then fixed in 10% formalin and prepared for routine histological examination. To determine the degree of collagen fiber accumulation, we randomly selected 20 fields in three individual sections and calculated the ratio of the areas of van Gieson-stained interstitial fibrosis to the total left ventricular area using image analysis software and a Zeiss KS400 system; perivascular fibrosis was excluded in the present study.

mRNA analysis

Total mRNA was prepared from the left ventricle using TRIzol (Life Technologies Inc., Rockville, MD). Expression of mRNAs encoding atrial natriuretic peptide (ANP), brain natriuretic peptide (BNP), collagens I and III, TGF-β1, TGF-β3, angiotensinogen (Agt), and Ang converting enzyme (ACE) was evaluated using quantitative RT-PCR in a 7700 sequence detector (ABI PRISM, Applied Biosystems, Foster City, CA). The oligonucleotide primers are shown in Table 1. Glyceraldehyde-3-phosphate dehydrogenase mRNA was also amplified with specific primers and probe (Applied Biosystems).

Experimental protocols

We first compared the gender-related differences in the phenotypes of 16-wk-old GC-A KO and WT mice (n = 7–9 per group). HR and SBP were measured, and LVW, LVW/BW, and left ventricular fibrosis were calculated, after which related mRNA expression was analyzed.

To evaluate the involvement of estrogen in gender-related differences, we compared the phenotypes of sham-operated and ovariectomized (OVX) mice (n = 7–9 per group). Under anesthesia with ether, the ovaries of 10-wk-old female mice were exteriorized, ligated, and removed *via* bilateral paralumbar incisions, which were then closed with sutures. In sham mice, the ovaries were exteriorized and replaced, and the incisions were closed. Six weeks later, HR and SBP were measured, and the animals were killed.

To investigate the effects of androgens, male mice at 10 wk of age (n = 7–9 per group) were castrated using the trans-scrotal approach. Sham castration consisted of exteriorizing and replacing the testes. As in females, 6 wk later, HR and SBP were measured, and the animals were killed.

To confirm the role of androgen, we ovariectomized female WT and GC-A KO mice (n = 6–7 per group) under anesthesia with ether at 10 wk of age and sc implanted a testosterone pellet (25.0 mg/pellet, 60-darelease, catalog item SA-151) or vehicle pellet (placebo for testosterone, catalog item SC-111) (Innovative Research of America, Sarasota, FL) between the shoulders. Six weeks later, the animals were killed after HR and SBP were measured.

We further confirmed the role of androgens by chronically blocking AR with flutamide (23–24). Flutamide (Sigma Chemical Co., St. Louis, MO; 8 mg/kg·d, dissolved in polyethylene glycol 300) was sc infused for 6 wk using an osmotic mini-pump (model 2002, Alza Corp., Mountain View, CA) at 10 wk of age in male animals (n = 7–9 per group). The mini-pumps were sc implanted under the mice were anesthetized with

TABLE 1. Primer and probe sequences for RT-PCR assays

mRNA	Probe	Primers[a]
ANP	TGTACAGTGCGGTGTCCAACACAGAT	*f*GCCATATTGGAGCAAATCCT
		*r*GCAGGTTCTTGAAATCCATCA
BNP	TGCAGAAGCTGCTGGAGCTGATAAGA	*f*CCAGTCTCCAGAGCAATTCAA
		*r*GCCATTTCCTCCGACTTTT
AT1A	CCGGAATTCAACGCTCCCCA	*f*GTTTGCGCTTTTCATTACGAGT
		*r*TCTTGGTTAGGCCCAGTCCT
ACE	CACATCCCAAACGTGACACCGTACAT	*f*CGGAATGAAACCCATTTTGA
		*r*GCACAAAGCTCACGAAGTACC
Agt	AGGTTCTCAATAGCATCCTCCTCGAACTC	*f*CATTGGTGACACCAACCCC
		*r*GCTGTTCCTCCTCTCCTGCT
TGF-β1	AGCGCATCGAAGCCATCCG	*f*GACGTCACTGGAGTTGTACGG
		*r*GCTGAATCGAAAGCCCTGT
TGF-β3	CGGATGAGCACATAGCCAAGCA	*f*TTGAGCTCTTCCAGATACTTCG
		*r*TTCTTGCCACCTATGTAGCG
Collagen I	CACGGCTGTGTGCGATGACG	*f*GTCCCAACCCCCAAAGAC
		*r*CATCTTCTGAGTTTGGTGATACGT
Collagen III	TCCCACTCTTATTTTGGCACAGCAGTC	*f*TGGTTTCTTCTCACCCTTCTTC
		*r*TGCATCCCAATTCATCTACGT

Sequences are listed 5′ to 3′.
[a] Forward primers are designated by *f* and reverse primers by *r*.

ether and changed with new ones every 2 wk. Control mice were administered only vehicle. Six weeks later, the animals were analyzed.

To assess the involvement of the AT1A receptors in GC-A disruption-induced gender difference, we deleted AT1A receptor by the described method above. At 16 wk of age, the animals (n = 5–9 per group) were analyzed.

To further support the conclusion of AT1A receptor involvement, we castrated male double-KO mice (10 wk old; n = 5–6 per group) and chronically infused exogenous testosterone and analyzed the animals by the described methods above.

Statistical analysis

All results are expressed as means ± SEM. Data were analyzed by one-facter ANOVA. If a statistically significant effect was found, the Newman-Keuls test was performed to isolate the difference between the groups. Values of $P < 0.05$ were considered statistically significant.

Results

GC-A deficiency induces gender-related cardiac differences

Targeted deletion of GC-A led to increased LVW/BW ratios in both male and female mice. However, the effect was greater in males (58% increase *vs.* 33% increase in females; Fig. 1A). In contrast, in WT mice, there was no difference in LVW/BW ratio in males *vs.* females (Fig. 1A). In addition, male GC-A KO mice, but not WT mice, exhibited higher levels of left ventricular fibrosis than did females (378% *vs.* 44%, respectively; Fig. 1, B and C). On the other hand, there was no gender-related difference in HR (WT female 599.6 ± 26.1 *vs.* male 619.0 ± 52.4 beats/min; GC-A KO female 574.5 ± 25.9 *vs.* male 571.3 ± 28.1 beats/min; n = 7–9 per group) or in SBP (WT female 118.4 ± 1.7 *vs.* male 113.2 ± 3.4 mm Hg; GC-A KO female 140.0 ± 3.4 *vs.* male 147.4 ± 2.2 mm Hg; n = 7–9 per group) in either genotype. Male mice weighed more than females, but there was no difference between genotypes [WT female 25.0 ± 0.9 *vs.* male 32.3 ± 1.6 g ($P < 0.05$); GC-A KO female 25.1 ± 0.8 *vs.* male 31.6 ± 1.9 g ($P < 0.05$); n = 7–9 per group].

OVX has little effect in the heart

To elucidate a possible mechanism by which GC-A could prevent gender-related difference in the heart, we first investigated the effects of estrogen depletion. OVX had no effect on HR (WT sham 599.6 ± 26.1 *vs.* OVX 590.4 ± 17.9 beats/min; GC-A KO sham 574.5 ± 25.9 *vs.* OVX 582.3 ± 14.1 beats/min; n = 7–9 per group), SBP (WT sham 118.4 ± 1.7 *vs.* OVX 112.0 ± 2.2 mm Hg; GC-A KO sham 140.6 ± 3.4 *vs.* OVX 137.7 ± 3.0 mm Hg; n = 7–9 per group), LVW/BW ratio, ventricular fibrosis in either mouse type (Fig. 1, A–C), or BW (WT sham 25.0 ± 0.9 *vs.* OVX 25.6 ± 0.8 g; GC-A KO sham 25.1 ± 0.8 *vs.* OVX 25.1 ± 1.6 g; n = 7–9 per group).

Neither castration nor administration of an AR antagonist diminishes cardiac hypertrophy and fibrosis in male GC-A KO mice, whereas testosterone infusion increases cardiac hypertrophy and fibrosis in OVX GC-A mice

In contrast to OVX, removal of testes was associated with a marked reduction in the LVW/BW ratio and in ventricular fibrosis in GC-A KO mice (by 20.5 and 44.7%, respectively) but not to levels comparable to those seen in WT mice. Castration had no effect in WT mice (Fig. 1). Castration reduced BW in male WT as well as in male GC-A KO mice [WT 5.7 ± 0.5 *vs.* 2.1 ± 0.4 g ($P < 0.05$), and GC-A KO 6.6 ± 0.9 *vs.* 2.7 ± 0.6 g ($P < 0.05$) for sham and castrated groups, respectively; n = 7–9 per group]. Castration had no effect on HR (WT 619.0 ± 52.4 *vs.* 606.2 ± 45.9 beats/min, and GC-A KO 571.3 ± 28.1 *vs.* 600.2 ± 13.2 beats/min, for sham and castrated groups, respectively; n = 7–9 per group) or SBP

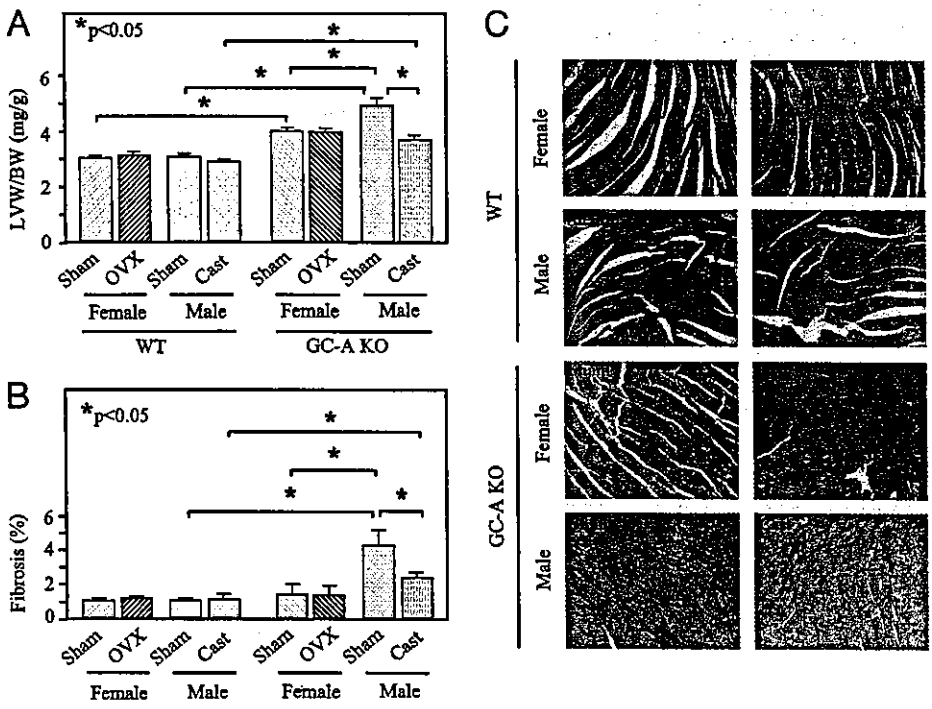

FIG. 1. GC-A disruption-induced gender-related differences in cardiac hypertrophy and fibrosis were inhibited by castration in male (Cast), but not in female (OVX) mice that were castrated at 10 wk and analyzed at 16 wk of age. The ratio of the areas of van Gieson-stained interstitial fibrosis to the total left ventricular area was calculated using image analysis software and a Zeiss KS400 system. A, LVW/BW ratio; B, relative levels of left ventricular fibrosis; C, photomicrographs showing representative examples of cardiac fibrosis (red) (magnification, ×200). Values are means ± SEM; n = 7–9 per group; *, $P < 0.05$.

(WT 113.2 ± 3.4 *vs.* 105.8 ± 4.2 mm Hg, and GC-A KO 147.4 ± 2.2 *vs.* 142.2 ± 6.3 mm Hg, for sham and castrated groups, respectively; n = 7–9 per group). The AR antagonist flutamide had similar effects to castration on LVW/BW, fibrosis (Fig. 2), HR (data not shown), and SBP (data not shown). In contrast, chronic infusion of testosterone increased LVW/BW ratio (by 20%) and cardiac fibrosis (by 114%) in OVX GC-A mice but not in OVX WT mice (Fig. 3). Testosterone treatment was also associated with increased BW in GC-A KO but not in WT mice JWT 2.6 ± 0.3 *vs.* 3.2 ± 0.3 g ($P < 0.05$), and GC-A KO 2.9 ± 0.2 *vs.* 5.2 ± 0.5 g ($P < 0.05$), for sham and testosterone-treated groups, respectively; n = 6–9 in each group[. HR and SBP were not affected by testosterone treatment (data not shown).

Gender-related difference in molecular expression profile

Basal left ventricular levels of ANP, BNP, collagen I, collagen III, TGF-β1, and TGF-β3 mRNAs were all higher in male than female GC-A KO mice. Castration of males decreased mRNA expression of these molecules to levels seen in females (Fig. 4). Again, no gender-related difference or castration-associated effects were seen in WT mice (Fig. 4). In contrast to the above mentioned genes, the levels of Agt and ACE mRNAs were higher in males than in females, and castration of males strongly suppressed their expression, and their levels were comparable in both genotypes of mice.

Deletion of AT1A abolishes gender-related cardiac differences

Deletion of the AT1A gene in GC-A KO mice reduced LVW/BW in both male and female mice, but the effects were more pronounced in the males (by 34 and 32.7% in males *vs.* 18 and 23.5% in females, respectively). AT1A deletion also markedly reduced cardiac fibrosis in male GC-A KO mice (by 57.5%). Gender-related cardiac differences (LVW/BW and fibrosis) were evident only in GC-A KO mice, but not in WT (as above), AT1A KO or double-KO mice (Fig. 5).

Castration or testosterone infusion fails to induce changes in cardiac mass and fibrosis in male double-KO mice

In contrast to the data obtained in GC-A KO mice (see above), neither castration nor testosterone infusion affected cardiac mass or the level of fibrosis in male double-KO mice (data not shown). Similarly, HR and SBP were unaffected by either castration or testosterone replacement (data not shown).

Discussion

As previous literatures documented significant gender-related differences in cardiovascular function and geometry (6, 7), the present study demonstrates that male GC-A KO mice show more marked left ventricular hypertrophy and severe interstitial fibrosis than female ones. Considering the protective effects of estrogen on the cardiovascular system (25, 26), we first investigated the effects of estrogens on the gender-related difference in the GC-A KO mouse hearts. Although OVX had little effect on cardiac mass and fibrosis in both WT and GC-A KO mice, there are still some possibilities that have not been addressed, such as, first, the fact that the effects of estrogen deprivation in women are not immediate; they develop over years, meaning that the 6-wk period of estrogen deprivation may be insufficient. Second, phytoestrogens are found in over 300 plants, including some used in human and animal diets (27–29). They can bind to the estrogen receptor and induce estrogen-like effects in animals, humans, and cells in culture. In the present study, we cannot exclude the possibility that the chow of mice may contain phytoestrogens, which may protect from (or limit) the effects of OVX. Therefore, the role of estrogen in gender-related cardiac difference observed in GC-A KO mice should be further clarified.

Next, we examined the effects of androgens. ARs are widely distributed in the cardiovascular system, where they have been identified on aortic, peripheral vascular, ventricular, and atrial myocytes (30), and were recently shown to mediate robust, testosterone-induced hypertrophic responses in cardiac myocytes (12). Nevertheless, although virtually all men have much higher levels of androgens than women do, not all men exhibit more severe cardiac hypertrophy and fibrosis. In the present study, significant gender-related differences in cardiac abnormalities were observed only in GC-A KO mice. In addition, it is notable that both castration and AR antagonist markedly diminished cardiac hypertrophy and fibrosis in male GC-A KO mice, and chronic

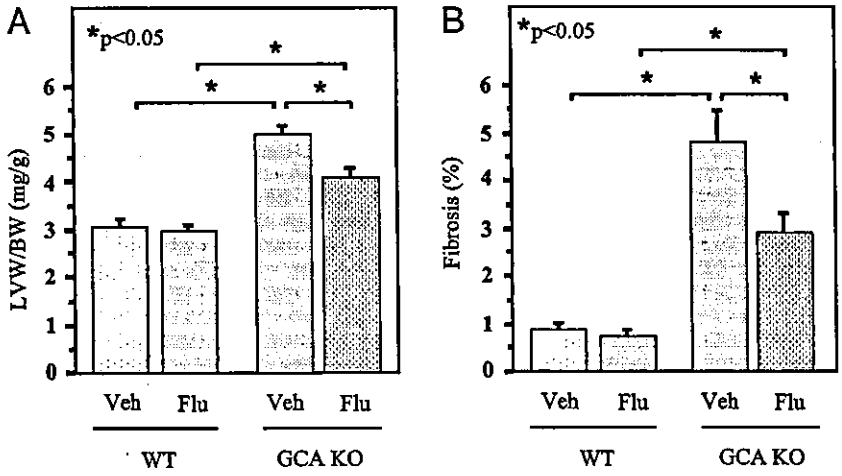

FIG. 2. Chronic AR blockade with flutamide was associated with decreased LVW/BW (A) and left ventricular fibrosis (B) in male GC-A KO mice. Flutamide (Flu; 8 mg/kg·d) or vehicle (Veh) was sc infused for 6 wk starting at 10 wk of age. Values are mean ± SEM; n = 7–9 per group; *, $P < 0.05$.

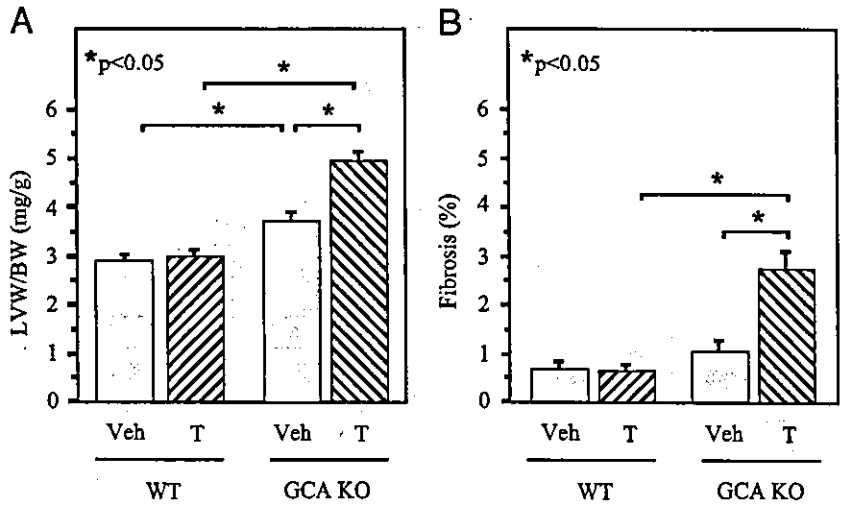

FIG. 3. Chronic infusion of testosterone (T) was associated with an increased LVW/BW (A) and left ventricular fibrosis (B) in OVX GC-A KO but not in OVX WT mice. A testosterone pellet (25.0 mg/pellet) or vehicle (Veh) was implanted sc at 10 wk of age, and 6 wk later, the animals were killed and analyses performed. Values are mean ± SEM; n = 6–7 per group; *, $P < 0.05$.

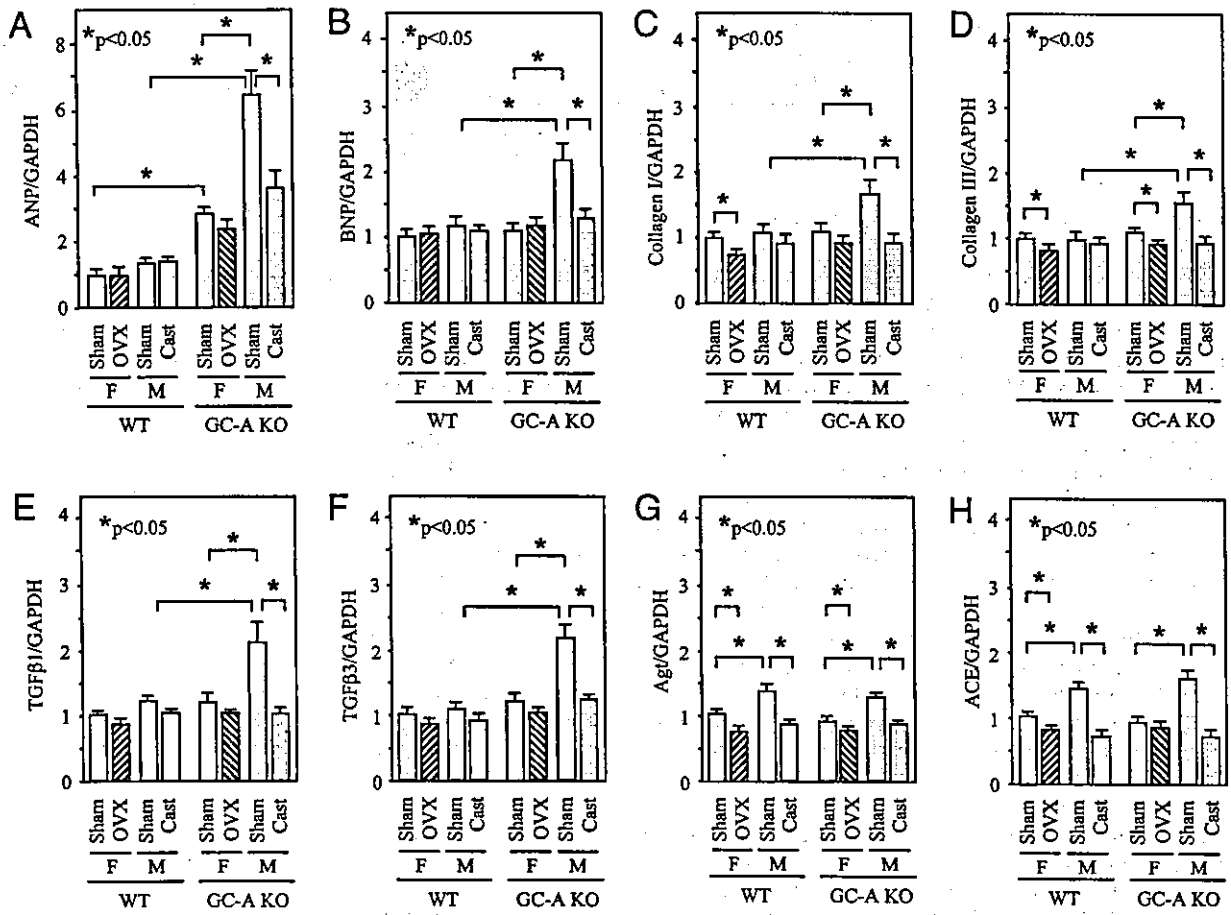

FIG. 4. Left ventricular levels of ANP, BNP, collagen I, collagen III, TGF-β1, and TGF-β3 mRNAs were elevated in male (M) GC-A KO mice and were reduced by castration to levels seen in females (F). Enhanced levels of Agt and ACE expression in male WT and GC-A KO mice were suppressed by castration, and levels were comparable in both genotypes. mRNAs were evaluated using quantitative RT-PCR in a 7700 sequence detector (ABI PRISM). Levels in sham female WT mice were arbitrarily assigned a value of 1.0. A, ANP; B, BNP; C, collagen I; D, collagen III; E, TGF-β1; F, TGF-β3; G, Agt; H, ACE. Values are mean ± SEM; n = 7–9; *, $P < 0.05$.

testosterone infusion increased cardiac mass and fibrosis only in OVX GC-A KO mice. ANP and BNP are well established molecular markers for cardiac hypertrophy. It has been demonstrated that the testosterone metabolite dihydrotestosterone is able to increase ANP secretion from ventricular myocytes. An AR antagonist, cyproterone, abolished

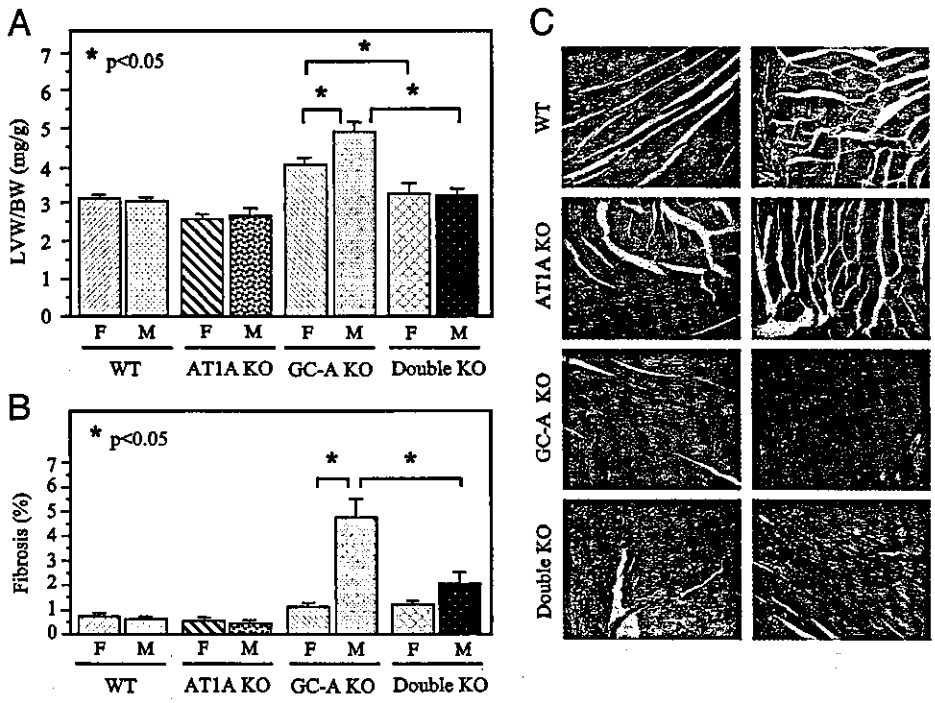

FIG. 5. Deletion of the AT1A receptor gene abolishes the gender-related differences in LVW/BW (A) and the relative levels of left ventricular fibrosis (B). C, Representative photomicrographs demonstrating fibrosis (red) in GC-A KO mice. Animals were analyzed at 16 wk of age. Values are mean ± SEM; n = 5–9 per group; *, $P < 0.05$.

this effect (12). Like cardiac geometric changes, changes in ANP and BNP, or markers for ventricular fibrosis, collagen I, and collagen III were higher in male GC-A KO mice than in females and were reduced by removal of testes. These findings suggest that androgens play an important role in gender-related cardiac differences in GC-A KO mice. Castration in males and AR antagonist could not reduce the cardiac mass and fibrosis to WT levels, suggesting that more than androgens are involved.

Ang II is known to potently stimulate cardiomyocyte and fibroblast growth, both *in vitro* and *in vivo* (31, 32), and the tissue renin-Ang system is known to play a key role in cardiac remodeling (33). It has been proposed that increased ACE abundance in the hypertrophied and failing heart may contribute to the local generation of Ang II and impact cardiac remodeling through local paracrine or autocrine effects (34–36). The greater abundance of ventricular ACE in males may contribute to the tendency of male rodents to develop cardiac abnormalities, which has been described in transgenic mouse models (37, 38) and spontaneously hypertensive rats (39) and in response to left ventricular pressure overload in rats (10) and in humans (40–42). It has been reported that hepatic Agt mRNA levels are higher in intact male hypertensive rats than in the females; moreover, those levels are reduced by orchidectomy and increased by administration of testosterone (43). Recently, Freshour *et al.* (44) demonstrated a gender difference in the expression of ACE in the murine heart with greater cardiac ACE levels seen in male animals compared with females. Moreover, ventricular ACE levels were substantially decreased in androgen-deprived males (44). Consistent with those reports, our data show that levels of cardiac Agt and ACE expression are higher in the ventricles of both GC-A KO and WT males than they are in females. Castration reduced expression of Agt in the male ventricle to levels approximating those seen in the females in both WT and GC-A KO mice. Given the evidence that Ang II has hypertrophic and fibrogenic activities in the heart, Ang II is a possible candidate to link androgens with cardiac abnormalities. It should be noted, however, that gender-related increases in LVW/BW ratios and interstitial fibrosis were observed only in the GC-A KO mice but not in WT mice, despite the similar up-regulation of Agt and ACE expression in ventricles of both genotypes of mice. We recently observed that GC-A signaling counteracts Ang II-induced cardiac abnormalities. A subpressor dose of Ang II increased cardiac mass and fibrosis only in male GC-A KO but not WT mice, suggesting an augmented responsiveness to Ang II in the heart of GC-A KO mice (22). Thus, we speculate that gender-related differences in the heart were made manifest by lacking inhibitory actions of GC-A on AT1 signaling in GC-A KO mice. Inhibitory effects of GC-A were also supported by the overexpression of TGF-β1 and -β3, which are activated by AT1A signaling and responsible for interstitial fibrosis (28, 45–47), in GC-A KO mice.

To further test this hypothesis, we deleted the AT1A receptor gene, which mediates classical Ang II actions, including cardiac hypertrophy and fibrosis, by crossing GC-A KO mice and AT1A KO mice. The gender-related cardiac differences were absent in the double-KO mice. Furthermore, castration of males did not reduce and testosterone administration failed to increase the cardiac mass and fibrosis in male double-KO mice. These results strongly suggest that GC-A prevents androgen-induced cardiac abnormalities mainly by inhibiting the androgen-Ang II-AT1A axis.

The present data did not indicate that androgens and Ang II solely provide a causative contribution to gender-related cardiac differences in GC-A KO mice. LVW/BW in male GC-A KO mice after castration or flutamide treatment were

comparable to that in female GC-A KO mice, but the degree of fibrosis was still higher in male GC-A KO mice after the treatments than in females, suggesting androgens mostly contribute to gender-related left ventricular hypertrophy, and at least approximately 50% to the gender-related increase in fibrosis. In the case of AT1A blockade, LVW/BW in GC-A KO mice were reduced to the level corresponding to that in WT mice, in which there was no difference in hypertrophy, and fibrosis was more intensively reduced by knocking out the AT1A receptor, compared with blockade of ARs. These findings suggest that AT1A signaling contributes not only to gender-related cardiac abnormalities but also to abnormalities specifically observed in both genders of GC-A KO mice, suggesting androgen is one of the factors up-regulating the Ang system. Additional studies are required to elucidate the entire mechanism for gender-related difference observed in GC-A KO mice, in which other molecules, such as catecholamines and endothelin, would be involved.

Another interesting finding is that castration or the treatment with androgen antagonist improved cardiac abnormalities in GC-A KO mice without significant change in SBP. As mentioned above, a subpressor dose of Ang II exaggerated hypertrophy and fibrosis in GC-A KO mice (22). It is likely, therefore, that androgen-induced Ang II is sufficient for inducing hypertrophy and fibrosis in GC-A KO mice but not to elevate BP.

The presence or absence of androgens in male GC-A KO mice showed marked effects on the expression levels of ANP. The molecular mechanism is unclear at present. In the present study, despite the similar up-regulation of Agt and ACE expression in ventricles of both male WT and GC-A KO mice, ANP was markedly increased only in male GC-A KO mice. We demonstrated a similar expression level of AT1A mRNA in males and females of both WT and GC-A KO mice (data not shown). Therefore, it seems that androgen-induced intracellular signaling at a postreceptor level for modulation of ANP gene expression is up-regulated in GC-A KO mice. Ang II is known to increase ANP expression mediated by protein kinase C or MAPK (48). Further examination is necessary to determine whether the protein kinase C or MAPK pathway is involved in the elevation of ANP by androgens.

Recently, Nakayama *et al.* (49) described a functional mutation in the 5′-flanking region of the human GC-A gene that reduces transcriptional activity by more than 70% in reporter gene assay, is present in approximately 5% of the hypertensive individuals in Japan, and is associated with cardiac hypertrophy. Evidence also suggests that GC-A receptors may be down-regulated in patients with chronic, severe heart failure (50). Indeed, there may be substantial numbers of patients whose abnormal GC-A signaling makes them susceptible to androgen-induced cardiac abnormalities. From the clinical points of view, the present study raises the possibility of the prophylactic use of Ang II receptor blocker or AR antagonist in patients with loss of functional mutations in the GC-A gene.

Taken together, our findings strongly support the hypothesis that androgen contributes to cardiac abnormalities *via* the AT1A receptor. Furthermore, this androgenic effect is normally inhibited by stimulation of GC-A by natriuretic peptides.

Acknowledgments

We thank Ms. Makoto Mukai and Ms. Itone Makino for their excellent secretarial assistance and Ms. Mika Inoue for her technical assistance. Dr. Yuhao Li is a foreign research fellow of the Japan Society for the Promotion of Science.

Received June 30, 2003. Accepted October 22, 2003.

Address all correspondence and requests for reprints to: Yoshihiko Saito, First Department of Internal Medicine, Nara Medical University, 840, Shijo-cho, Kashihara, Nara 634-8522, Japan. E-mail: yssaito@naramed-u.ac.jp.

This work was supported in part by research grants from Japanese Ministry of Education, Science and Culture, the Japanese Ministry of Health and Welfare, the Japanese Society for the Promotion of Science Research for the Future program (JSPS-RFTF96I00204 and JSPS-RFTF98L00801), the Uehara Memorial Foundation, the Smoking Research Foundation, and the Howard Hughes Medical Institute.

References

1. **Devereux RB, Pickering TG, Alderman MH, Chien S, Borer JS, Laragh JH** 1987 Left ventricular hypertrophy in hypertension: prevalence and relationship to pathophysiologic variables. Hypertension 9(Suppl II):53–60
2. **Kaplinsky E** 1994 Significance of left ventricular hypertrophy in cardiovascular morbidity and mortality. Cardiovasc Drugs Ther 8:549–556
3. **Neyses L, Pelzer T** 1995 The biological cascade leading to cardiac hypertrophy. Eur Heart J 16(Suppl N):8–11
4. **Weber KT, Brilla CG** 1991 Pathological hypertrophy and cardiac interstitium. Fibrosis and renin-angiotensin-aldosterone system. Circulation 83:1849–1865
5. **Hayward CS, Kelly RP, Collins P** 2000 The roles of gender, the menopause and hormone replacement on cardiovascular function. Cardiovasc Res 46: 28–49
6. **Fiebach NH, Viscoli CM, Horwitz RI** 1990 Differences between women and men in survival after myocardial infarction. JAMA 263:1092–1096
7. **de Simone G, Devereux RB, Daniels SR, Meyer RA** 1995 Gender differences in ventricular growth. Hypertension 26:979–983
8. **Luchner A, Brockel U, Muscholl M, Hense HW, Doring A, Riegger GA, Schunkert H** 2002 Gender-specific differences of cardiac remodeling in subjects with left ventricular dysfunction: a population-based study. Cardiovasc Res 53:720–727
9. **Crabbe DL, Dipla K, Ambati S, Zafeiridis A, Gaughan JP, Houser SR, Margulies KB** 2003 Gender differences in post-infarction hypertrophy in end-stage failing hearts. J Am Coll Cardiol 41:300–306
10. **Weinberg EO, Thienelt CD, Katz SE, Bartunek J, Tajima M, Rohrbach S, Douglas PS, Lorell BH** 1999 Gender differences in molecular remodeling in pressure overload hypertrophy. J Am Coll Cardiol 34:264–273
11. **Meyer R, Linz KW, Surges R, Meinardus S, Vees J, Hoffmann A, Windholz O, Grohe C** 1998 Rapid modulation of L-type calcium current by acutely applied oestrogens in isolated cardiac myocytes from human, guinea-pig and rat. Exp Physiol 83:305–321
12. **Marsh JD, Lehmann MH, Ritchie RH, Gwathmey JK, Green GE, Schiebinger RJ** 1998 Androgen receptors mediate hypertrophy in cardiac myocytes. Circulation 98:256–261
13. **Dubey RK, Gillespie DC, Jackson EK, Keller PJ** 1998 17β-Estradiol, its metabolites, and progesterone inhibit cardiac fibroblast growth. Hypertension 31:522–528
14. **Chen SJ, Li H, Durand J, Oparil S, Chen YF** 1996 estrogen reduces myointimal proliferation after balloon injury of rat carotid artery. Circulation 93:577–584
15. **Somjen D, Kohen F, Jaffe A, Amir-Zaltsman Y, Knoll E, Stern N** 1998 Effect of gonadal steroids and their antagonists on DNA synthesis in human vascular cells. Hypertension 32:39–45
16. **Fujimoto R, Morimoto I, Morita E, Sugimoto H, Ito Y, Eto S** 1994 Androgen receptors, 5α-reductase activity and androgen-dependent proliferation of vascular smooth muscle cells. J Steroid Biochem Mol Biol 50:169–174
17. **Cabral AM, Vasquez EC, Moyses MR, Antonio A** 1988 Sex hormone modulation of ventricular hypertrophy in sinoaortic denervated rats. Hypertension 11:193–197
18. **Malhotra A, Buttrick P, Scheuer J** 1990 Effects of sex hormones on development of physiological and pathological cardiac hypertrophy in male and female rats. Am J Physiol 259:H866–H871
19. **Lopez MJ, Wong SK, Kishimoto I, Dubois S, Mach V, Friesen J, Garbers DL, Beuve A** 1995 Salt-resistant hypertension in mice lacking the guanylyl cyclase-A receptor for atrial natriuretic peptide. Nature 378:65–68
20. **Oliver PM, Fox JE, Kim R, Rockman HA, Kim HS, Reddick RL, Pandey KN, Milgram SL, Smithies O, Maeda N** 1997 Hypertension, cardiac hypertrophy, and sudden death in mice lacking natriuretic peptide receptor A. Proc Natl Acad Sci USA 94:14731–14735
21. **Sugaya T, Nishimatsu S, Tanimoto K, Takimoto E, Yamagishi T, Imamura K, Goto S, Imaizumi K, Hisada Y, Otsuka A, Uchida H, Sugiura M, Fukuta**

K, Fukamizu A, Murakami K 1995 Angiotensin II type 1a receptor-deficient mice with hypotension and hyperreninemia. J Biol Chem 270:18719–18722
22. Li Y, Kishimoto I, Saito Y, Harada M, Kuwahara K, Izumi T, Takahashi N, Kawakami R, Tanimoto K, Nakagawa Y, Nakanishi M, Adachi Y, Garbers DL, Fukamizu A, Nakao K 2002 Guanylyl cyclase-A inhibits angiotensin II type 1A receptor-mediated cardiac remodeling, an endogenous protective mechanism in the heart. Circulation 106:1722–1728
23. Labrie F 1993 Mechanisms of action and pure antiandrogenic properties of flutamide. Cancer 72:3816–3827
24. Reckelhoff JF, Zhang H, Srivastava K, Granger JP 1999 Gender differences in hypertension in spontaneously hypertensive rats: role of androgens and androgen receptor. Hypertension 34:920–923
25. Mendelsohn ME, Karas RH 1999 The protective effects of estrogen on the cardiovascular system. N Engl J Med 340:1801–1811
26. van Eickels M, Grohe C, Cleutjens JP, Janssen BJ, Wellens HJ, Doevendans PA 2001 17β-Estradiol attenuates the development of pressure-overload hypertrophy. Circulation 104:1419–1423
27. Farnsworth NR, Bingel AS, Cordell GA, Crane FA, Fong HHS 1975 Potential value of plants as sources of new antifertility agents. J Pharm Sci 64:717–754
28. Price KR, Fenwick GR 1985 Naturally occurring oestrogens in foods: a review. Food Addit Contam 2:73–106
29. Degen GH, Janning P, Diel P, Bolt HM 2002 Estrogenic isoflavones in rodent diets. Toxicol Lett 128:145–157
30. Mcgill HC, Sheridan PJ 1981 Nuclear uptake of sex steroid hormones in the cardiovascular system of the baboon. Circ Res 48:238–244
31. Sadoshima J, Izumo S 1993 Molecular characterization of angiotensin II-induced hypertrophy of cardiac myocytes and hyperplasia of cardiac fibroblasts. Critical role of AT1 receptor subtype. Circ Res 73:413–423
32. Schorb W, Booz GW, Dostal DE, Conrad KM, Chang KC, Baker KM 1993 Angiotensin II is mitogenic in neonatal rat cardiac fibroblasts. Circ Res 72: 1245–1254
33. McDonald KM, Garr M, Carlyle PF, Francis GS, Hauer K, Hunter DW, Parish T, Stillman A, Cohn JN 1999 Relative effects of α1-adrenergic blockade, converting enzyme inhibitor therapy, and angiotensin II subtype 1 receptor blockade on ventricular remodeling in the dog. Circulation 90:3034–3046
34. Bader M, Peters J, Baltatu O, Muller DN, Luft FC, Ganten D 2001 Tissue rennin-angiotensin systems: new insights from experimental animal models in hypertensive research. J Mol Med 79:76–102
35. Pratt RE 1999 Angiotensin II and the control of cardiovascular structure. J Am Soc Nephrol 10:S120–S128
36. Weber KT 1997 Extra cellular matrix remodeling in heart failure. A role for de novo angiotensin II generation. Circulation 96:4065–4082
37. Kadokami T, McTiernan CF, Kubota T, Frye CS, Feldman AM 2000 Sex-related survival differences in murine cardiomyopathy are associated with differences in TNF-receptor expression. J Clin Invest 106:589–597
38. Vikstrom KL, Factor SM, Leinwand LA 1996 Mice expressing mutant myosin are a model for hypertrophic cardiomyopathy. Mol Med 2:556–567
39. Wallen WJ, Cserti C, Belanger MP, Wittnich C 2000 Gender-differences in myocardial adaptation to afterload in normotensive and hypertensive rats. Hypertension 36:774–779
40. Carroll JD, Carroll EP, Feldman T, Ward DM, Lang RM, McGaughey D, Karp RB 1992 Sex-associated differences in left ventricular function in aortic stenosis of the elderly. Circulation 86:1099–1107
41. Douglas PS, Katz SE, Weinberg EO, Chen MH, Bishop SP, Lorell BH 1998 Hypertrophic remodeling: gender differences in the early response to left ventricular pressure overload. J Am Coll Cardiol 32:1118–1125
42. Villarreal FJ, Dillmann WH 1992 Cardiac hypertrophy-induced changes in mRNA levels for TGF-β1, fibronectin, and collagen. Am J Physiol Heart Circ Physiol 262:H1861–H1866
43. Chen YF, Naftilan AJ, Oparil S 1992 Androgen-dependent angiotensinogen and renin messenger RNA expression in hypertensive rats. Hypertension 19:456–463
44. Freshour JR, Chase SE, Vikstrom KL 2002 Gender differences in cardiac ACE expression are normalized in androgen-deprived male mice. Am J Physiol Heart Circ Physiol 283:H1997–H2003
45. Border WA, Nobel NA 1994 Transforming growth factor-β in tissue fibrosis. N Engl J Med 331:1286–1292
46. Kagami S, Border WA, Miller DE, Noble NA 1994 Angiotensin II stimulates extracellular matrix protein synthesis through induction of transforming growth factor-β expression in rat glomerular mesangial cells. J Clin Invest 93:2431–2437
47. Johnston CI, Hodsman PG, Kohzuki M, Casley DJ, Fabris B, Phillips PA 1989 Interaction between atrial natriuretic peptide and the renin angiotensin aldosterone system. Am J Med 87:24S–28S
48. Sadoshima J, Izumo S 1997 The cellular and molecular response of cardiac myocytes to mechanical stress. Annu Rev Physiol 59:551–571
49. Nakayama T, Soma M, Takahashi Y, Rehemudula D, Kanmatsuse K, Furuya K 2000 Functional deletion mutation of the 5′-flanking region of type A human natriuretic peptide receptor gene and its association with essential hypertension and left ventricular hypertrophy in the Japanese. Circ Res 86:841–845
50. Tsutamoto T, Kanamori T, Morigami N, Sugimoto Y, Yamaoka O, Kinoshita M 1993 Possibility of down-regulation of atrial natriuretic peptide receptor coupled to guanylate cyclase in peripheral vascular beds of patients with chronic severe heart failure. Circulation 88:811–813

Endocrinology is published monthly by The Endocrine Society (http://www.endo-society.org), the foremost professional society serving the endocrine community.

Available online at www.sciencedirect.com

SCIENCE DIRECT

Regulatory Peptides 128 (2005) 7–13

REGULATORY PEPTIDES

www.elsevier.com/locate/regpep

Chronic administration of adrenomedullin attenuates the hypertension and increases renal nitric oxide synthase in Dahl salt-sensitive rats

Fumiki Yoshihara[a,*], Shin-ichi Suga[b], Naomi Yasui[b], Takeshi Horio[a], Takeshi Tokudome[b], Toshio Nishikimi[c], Yuhei Kawano[a], Kenji Kangawa[b]

[a]*Division of Hypertension and Nephrology, National Cardiovascular center, 5-7-1 Fujishirodai, Suita, Osaka 565-8565, Japan*
[b]*National Cardiovascular Center Research Institute, 5-7-1 Fujishirodai, Suita, Osaka 565-8565, Japan*
[c]*Department of Hypertension and Cardiorenal Medicine, Dokkyo University School of Medicine, Mibu, Tochigi 321-0293, Japan*

Received 16 June 2004; accepted 10 December 2004
Available online 27 January 2005

Abstract

Adrenomedullin reduces systemic blood pressure and increases urinary sodium excretion partly through the release of nitric oxide. We hypothesized that chronic adrenomedullin infusion ameliorates salt-sensitive hypertension and increases the expression of renal nitric oxide synthase (NOS) in Dahl salt-sensitive (DS) rats, because the reduced renal NOS expression promotes salt sensitivity. DS rats and Dahl salt-resistant (DR) rats were fed a high sodium diet (8.0% NaCl) for 3 weeks. The high sodium diet resulted in an increase in blood pressure and a reduction of urinary sodium excretion in association with increased renal adrenomedullin concentrations and decreased expression of renal neuronal NOS (nNOS) and renal medullary endothelial NOS (eNOS) in DS rats compared with DR rats. Chronic adrenomedullin infusion partly inhibited the increase of blood pressure and proteinuria in association with a restoration of renal nNOS and medullary eNOS expression in DS rats under the high sodium diet. The immunohistochemical analysis revealed that the restored renal nNOS expression induced by chronic adrenomedullin infusion may reflect the restoration of nNOS expression in the macula densa and inner medullary collecting duct. These results suggest that adrenomedullin infusion has beneficial effects on this hypertension probably in part through restored renal NOS expression in DS rats.

Keywords: Adrenomedullin; Kidney; Nitric oxide synthase; Rats; Dahl; Western blot

1. Introduction

Salt sensitivity has been reported to be an independent cardiovascular risk factor in patients with hypertension [1], suggesting that the investigation of renal mechanisms of salt sensitivity is necessary to open up a possible new therapeutic strategy for hypertension. Nitric oxide (NO) was reported to stimulate an adaptive response to increased dietary sodium intake, cause vasodilation, and facilitate natriuresis [2]. The inhibition of nitric oxide synthase (NOS) was found to blunt the pressure–natriuresis relationship in normotensive rats [3], suggesting that an impaired NOS may be one of the factors causing salt-sensitive hypertension [4]. Furthermore, the reduced renal neuronal NOS (nNOS) activity in rats with salt-sensitive hypertension has been reported to promote salt sensitivity [5].

Adrenomedullin is a vasodilatory peptide originally discovered in human pheochromocytoma tissue [6]. Subsequent studies demonstrated that adrenomedullin and its specific binding sites are widely distributed in the cardiovascular system, including the kidney, heart, lungs and blood vessels [6,7]. Adrenomedullin immunoreactivity exists in glomeruli, cortical distal tubules, and medullary collecting duct cells [8]. These results suggest that adrenomedullin may play a role in the regulation of renal function. Indeed, intrarenal infusion of adrenomedullin increased the renal blood flow, glomerular filtration rate, renal sodium excretion [8]. Adrenomedullin also regulates

* Corresponding author. Tel.: +81 6 6833 5012; fax: +81 6 6872 7486.
E-mail address: fyoshi@ri.ncvc.go.jp (F. Yoshihara).

0167-0115/$ - see front matter © 2005 Elsevier B.V. All rights reserved.
doi:10.1016/j.regpep.2004.12.028

the NO production. Recently, adrenomedullin has been reported to induce NO production via the Ca^{2+}/calmodulin-dependent pathway in cultured endothelial cells [9]. These results suggested that adrenomedullin may participate in the regulation of NO production through the stimulation of eNOS and nNOS which are activated by calcium and calmodulin, and renal sodium excretion in rats with salt-sensitive hypertension.

We hypothesized that renal adrenomedullin participates in the regulation of salt sensitivity by modulating renal eNOS and nNOS, and that chronic adrenomedullin infusion ameliorates salt-sensitive hypertension and increases the expression of renal nitric oxide synthase (NOS) in Dahl salt-sensitive (DS) rats.

Thus, the purposes of this study were 1) to investigate whether the renal adrenomedullin level correlates with systemic blood pressure and urinary sodium excretion, 2) to examine whether adrenomedullin supplementation improves the salt-sensitive hypertension and affects the altered renal eNOS and nNOS expression, and 3) to evaluate where nNOS exists in the kidney in DS rats.

2. Materials and methods

2.1. Experimental animals

We used 6-week-old male DS rats and Dahl salt-resistant (DR) rats (Eisai Co. Ltd. Tokyo, Japan) in the present study. This study was performed in accordance with the guidelines of the Animal Care Committee of the National Cardiovascular Center Research Institute.

2.2. Protocol 1

The total experimental period was 4 weeks. The animals (DR rats: n=22, DS rats: n=23) were fed a regular sodium diet (0.5% NaCl) for 1 week followed by a high sodium diet (8.0% NaCl) for 3 weeks during our experimental protocol. The rats were sacrificed and the kidneys were excised for the analyses at the end of the 2nd-, 3rd-, and 4th-week of the study.

2.2.1. Urinary parameters

Twenty-four-hour urinary samples were collected from rats in metabolic cages at the end of the 1st-, 2nd-, 3rd-, and 4th-week of the study for the measurement of urinary volume and sodium excretion level. The urinary sodium level was measured by an auto-analyzer.

2.2.2. Blood pressure measurements

Systolic blood pressure was measured in conscious, restrained rats before the day of the urinary collection in every week by the tail cuff method with automated sphygmomanometers. Rats were placed in individual restrainers and pre-warmed at 37 °C. The average of three readings was recorded.

2.2.3. Measurements of renal tissue adrenomedulln

The rat adrenomedullin levels in the renal cortex and medulla were measured at the end of the 4th-week of the study in DS and DR rats. Radioimmunoassay for rat adrenomedullin was performed as described previously [10].

2.2.4. Western blot analysis

Western blotting for eNOS and nNOS in the renal cortex and medulla (DR rats, n=4; DS rats, n=4) was carried out at the end of the 4th-week of the study [11]. Twenty-microgram kidney tissue preparations were size-fractionated on 4–12% Tris-Glycine gel (Bio-Rad) at 200V for 1.5 h. After electrophoresis, proteins were transferred onto Immobilon-P membrane (Millipore) at 350 mA for 100 min. The membrane was prehybridized in 10 mL of TBST (10 mmol/L Tris hydrochloride, pH 7.5, 100 mmol/L NaCl, 0.1% Tween 20) containing 5% nonfat milk for 2 h and hybridized overnight in the same buffer containing anti-eNOS or anti-nNOS monoclonal antibodies (1:750, Transduction Labs). The membrane was then washed for 30 min with TBST and then incubated with TBST with 5% nonfat milk and goat anti-mouse IgG-horseradish peroxidase (1:1000, Amersham) After the washes, the membrane was developed with a chemiluminating method using ECL reagent (Amersham Inc). The membrane was then subjected to autoluminography for 5–10 min. The autoluminographs were scanned with a laser densitometer to determine the relative optical densities of the bands. The membranes were stained with India ink before prehybridization to confirm an equal amount of protein loading and transfer efficiency among the samples.

2.3. Protocol 2

The experimental period and the feeding protocol were identical to those of protocol 1. Before the 2nd-week, DS rats were randomly divided into 2 groups; the adrenomedullin-treated group and the untreated group. After pentobarbital sodium anesthesia (30 mg/kg, IP), the rats were subcutaneously implanted with an osmotic minipump (Model 2ML4, Alza) filled with recombinant human adrenomedullin dissolved in 0.9% saline in the adrenomedullin-treated group (DS-AM, 400 ng/hr per rat, n=14) and and 0.9% saline in the untreated group (DS-S, n=14). for evaluating the effects of adrenomedullin infusion on systolic blood pressure and urinary sodium excretion under the high sodium diet.

2.3.1. Recombinant human adrenomedullin

Recombinant human adrenomedullin was kindly provided by Shionogi Pharmaceutical, Osaka, Japan. Adrenomedullin with a glycine extension residue at the C-terminus (adrenomedullin-gly) was expressed in *Escherichia coli*. The product was digested with a site-specific protease after denaturation. The resulting adrenomedullin-gly was amidated by a peptidyl-glycine amidating enzyme for conversion to the mature form of adrenomedullin with an amidated C-terminus.

2.3.2. Urinary parameters, blood pressure measurements, and western blot analysis

Twenty-four-hour urinary samples were collected from rats in metabolic cages at the end of each week throughout the study for the measurement of urinary volume and protein excretion. Urinary sodium excretion was measured at the end of 4th-week. Systolic blood pressure was measured before the day of the urine collection. Western blot analysis for eNOS and nNOS in the renal cortex and medulla was performed at the end of protocol 2.

2.3.3. Immunohistochemistry

For immunohistochemical analysis, the kidneys were fixed with Methyl Carnoy. The tissues were embedded in paraffin, and 3-μm-thick sections were cut and mounted on glass slides treated with silica. An indirect immunoperoxidase method was used to identify the nNOS antigen (a mouse IgG to neuronal NOS, Transduction Labs) [12].

2.4. Statistical analysis

All values are presented as mean±SD. Comparisons of 3 or more groups were performed by ANOVA with the Scheffe's post hoc test. Comparisons between 2 groups were performed by the unpaired t test. Differences were considered statistically significant at a level of $p<0.05$. Correlation coefficients were calculated using linear regression analysis.

3. Results

3.1. Protocol 1

Body weight was significantly reduced and left ventricular plus septal weight was significantly increased at the 4th-week in DS rats compared with DR rats (Table 1). Kidney weight was also increased after the 3rd-week in DS rats compared with DR rats (Table 1). Systolic blood pressure and urinary sodium excretion were not significantly different between DS and DR rats at the 2nd-week (Table 1). While systolic blood pressure significantly increased after the 3rd-week, urinary sodium excretion decreased only at the 4th-week in DS rats compared with DR rats (Table 1).

Table 2
Correlations between renal adrenomedullin (AM) concentrations with urinary sodium excretion and systolic blood pressure at the 4th-week in protocol 1

	Cortical AM (fmol/mg)	Medullary AM (fmol/mg)
Urinary Na excretion (mmol/day)	$R=-0.68$, $p<0.01$	$R=-0.60$, $p<0.05$
Systolic Blood Pressure (mmHg)	$R=0.85$, $p<0.0001$	$R=0.86$, $p<0.0001$

The tissue adrenomedullin concentrations in both the renal cortex and medulla were significantly increased at the end of 4th-week in DS rats compared with DR rats (Table 1). The increased renal adrenomedullin levels in the renal cortex and medulla inversely correlated with urinary sodium excretion and positively correlated with systolic blood pressure (Table 2). Western blot analysis revealed that the eNOS expression in the renal medulla and the nNOS expression in both the renal cortex and medulla were significantly lower in DS rats compared with DR rats at the end of the 4th-week (Fig. 1). However, renal cortical eNOS expression was comparable between DS and DR rats (Fig. 1).

3.2. Protocol 2

The chronic adrenomedullin infusion did not affect body and kidney weight in DS rats, however, its infusion significantly reduced the left ventricular and septal weight in DS rats at the end of the 4th-week (Table 3). The chronic adrenomedullin infusion significantly reduced systolic blood pressure and tended to increase urinary sodium excretion at the 4th-week in DS rats under the high sodium diet (Table 3). Chronic adrenomedullin infusion signifi-

Table 1
Number, body weight, heart rate, heart and kidney weights in Dahl rats during feeding on the high sodium diet

	2nd-week		3rd-week		4th-week	
	DR	DS	DR	DS	DR	DS
N	7	8	8	7	7	8
BW (g)	286±16	292±9	309±11	297±14	371±12	342±12**
HR (bpm)	389±24	398±37	396±36	373±10	377±22	399±25
LV+SEP/BW (mg/g)	2.06±0.15	2.19±0.07	2.22±0.16	2.42±0.07	1.97±0.11	2.58±0.13[a]
Kid/BW (mg/g)	3.69±0.26	3.91±0.14	4.09±0.13	4.46±0.20*	3.67±0.13	4.64±0.19[a]
SBP (mmHg)	119±8	126±6	124±9	166±5[a]	125±8	169±7[a]
UNaV (mmol/day)	2.1±1.0	2.4±0.7	1.9±0.6	1.9±0.9	2.7±1.3	1.2±0.3**
Cortical AM (fmol/mg)	0.59±0.10	0.62±0.05	0.56±0.06	0.61±0.09	0.55±0.06	0.74±0.06**
Medullary AM (fmol/mg)	0.31±0.06	0.31±0.05	0.34±0.04	0.31±0.05	0.34±0.02	0.45±0.04**

N indicates number of rats; BW, body weight; HR, heart rate; LV+SEP, left ventricular and septal weight; Kid, kidney weight; SBP, systolic blood pressure; UNaV, urinary sodium excretion. Data are mean±SD.

[a] $p<0.0001$ vs DR at the same period, * $p<0.05$ vs DR, ** $p<0.01$ vs DR.

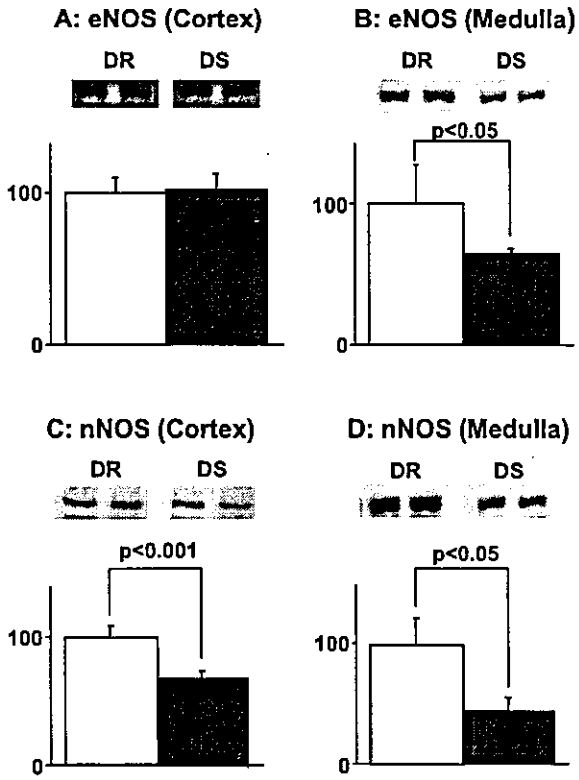

Fig. 1. Representative Western blots showing NOS and relative abundance of NOS in the renal cortex and medulla at the end of the 4th-week in Dahl rats in protocol 1 (n=4, in each group). A, B: eNOS; C,D: nNOS.

cantly restored eNOS expression in the renal medulla and nNOS expression in the renal cortex and medulla in DS rats at the end of the 4th-week (Fig. 2). Furthermore, the levels of proteinuria were significantly higher in DS rats than DR rats during all over the high sodium diet and chronic adrenomedullin infusion significantly inhibited the increasing of proteinuria levels under the high sodium diet in DS rats (Table 4). The immunohistochemical analysis revealed

Table 3
Number, body weight, heart rate, heart and kidney weights in Dahl rats treated with saline or adrenomedullin at the end of the 4th-week

	DR-S	DS-S	DS-AM
N	19	14	14
BW (g)	370±11	348±15*	350±14*
HR (bpm)	347±32	355±38	332±35
LV+SEP/BW (mg/g)	1.90±0.13	2.54±0.13*	2.32±0.14[a,*]
Kid/BW (mg/g)	3.85±0.28	4.63±0.26*	4.52±0.27*
SBP (mmHg)	128±6	173±10**	150±10[b,**]
UNaV (mmol/day)	2.2±0.7	1.4±0.5*	1.7±0.5

Abbreviations as in Table 1. DR-S indicates DR rats treated with saline; DS-S, DS rats treated with saline; DS-AM, DS rats treated with adrenomedullin. Data are mean±SD.

[a] p<0.001 vs DS-S.
[b] p<0.001 vs DS-S.
* p<0.001 vs DR-S.
** p<0.0001 vs DR-S.

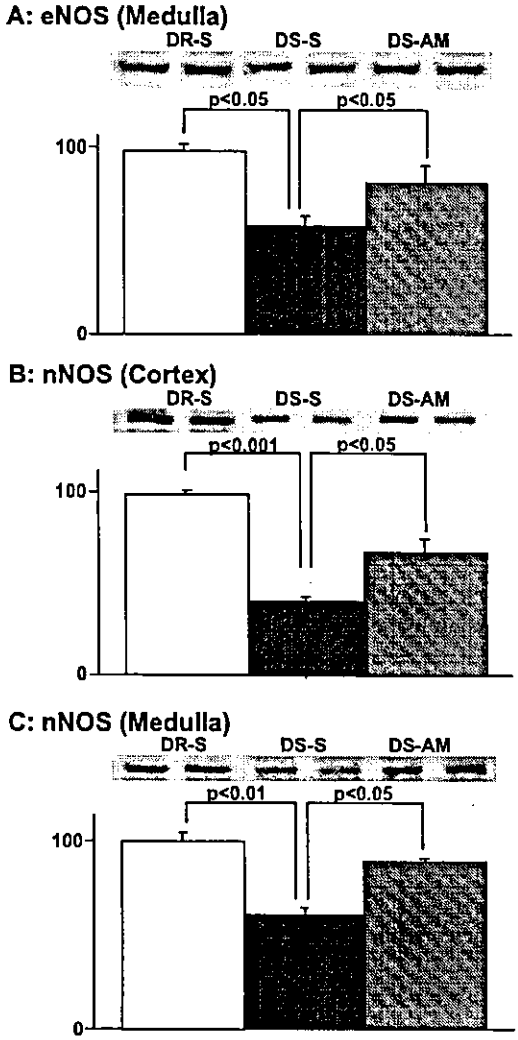

Fig. 2. The effect of chronic adrenomedullin infusion on the NOS expression in the renal cortex and medulla at the end of the 4th-week in protocol 2 (n=4, in each group). A: eNOS; B,C: nNOS.

that nNOS was localized in the macula densa and inner medullary collecting duct cells in all groups (Fig. 3).

4. Discussion

In the present study, we demonstrated for the first time that 1) the tissue adrenomedullin levels in the renal cortex and medulla significantly increased in DS rats compared with DR rats after 3 weeks on a high sodium diet, and were negatively correlated with urinary sodium excretion and positively correlated with systolic blood pressure, 2) the expression of eNOS in the renal medulla and nNOS in the renal cortex and medulla significantly reduced in DS rats, 3) chronic adrenomedullin supplementation significantly reduced systolic blood pressure, tended to increase urinary sodium excretion, and reduced urinary protein excretion in association with the restoration of renal medullary eNOS

Table 4
The effect of chronic adrenomedullin infusion on the levels of proteinuria during feeding on the high sodium diet in DS rats in protocol 2

Urinary protein (mg/day/100gBW)	2nd-week	3rd-week	4th-week
DR-S	3.4±1.1	3.2±0.9	3.4±0.9
DS-S	5.2±1.7*	6.5±2.5**	7.8±2.7**
DS-AM	3.5±1.0[b]	4.5±1.2[b]	5.7±1.6[a]

[a] $p<0.05$ vs DS-S.
[b] $p<0.01$ vs DS-S.
* $p<0.01$ vs DR-S.
** $p<0.0001$ vs DR-S.

and cortical and medullary nNOS expression, and 4) adrenomedullin may stimulate renal nNOS level in the macula densa and inner medullary collecting duct. These results suggest that chronic adrenomedullin infusion has beneficial effects on this hypertension probably in part through increased eNOS expression in renal medulla and nNOS expression in macula densa and inner medullary collecting duct in DS rats and that renal adrenomedullin may serve as an endogenous protective mechanism against salt-sensitive hypertension.

Adrenomedullin infusion has been reported not only to reduce systemic blood pressure in spontaneously hypertensive rats [13] and healthy human subjects [14], but also to increase urinary sodium excretion in anesthetized normal dogs [15]. These results suggested that adrenomedullin may regulate systemic blood pressure and urinary sodium excretion. However, the involvement of adrenomedullin has not been reported in the reduction of urinary sodium excretion that causes salt-sensitive hypertension in Dahl rats. Since we showed that the increased level of renal adrenomedullin correlated both with systemic blood pressure and urinary sodium excretion, there is a possibility that renal adrenomedullin is involved in the modulation of salt-sensitive hypertension in DS rats. Furthermore, chronic adrenomedullin infusion attenuated the increase of blood pressure and heart weight, suggesting that increased renal adrenomedullin may serve as an endogenous protective mechanism against salt-sensitive hypertension.

NO has been shown to play an important role in various physiological processes in the kidney, including sodium and fluid reabsorption [16], renal hemodynamics [17] and tubuloglomerular feedback [18]. Endogenous NO is enzymatically produced from the conversion of the amino acid L-arginine to L-citrulline, a reaction that is catalyzed by NOS. Three different NOS isoforms have been identified; namely a nNOS, a eNOS, and an inducible (iNOS) isoform, which are differentially expressed throughout the kidney [19]. Previous report demonstrated that renal eNOS activity was comparable between DS and DR rats under the high sodium diet [5]. We also compared the expression of eNOS protein in renal medulla and cortex, respectively between DS and DR rats. In the renal cortex eNOS expression had no significant difference between DS and DR rats after the 3-week high sodium diet. It was almost a similar result with the above report [5]. However, in the renal medulla eNOS expression was significantly reduced in DS rats compared with DR rats. Taken together with the fact that the inhibition of NOS causes salt-sensitive hypertension, the reduced eNOS expression in the renal medulla may be involved in part

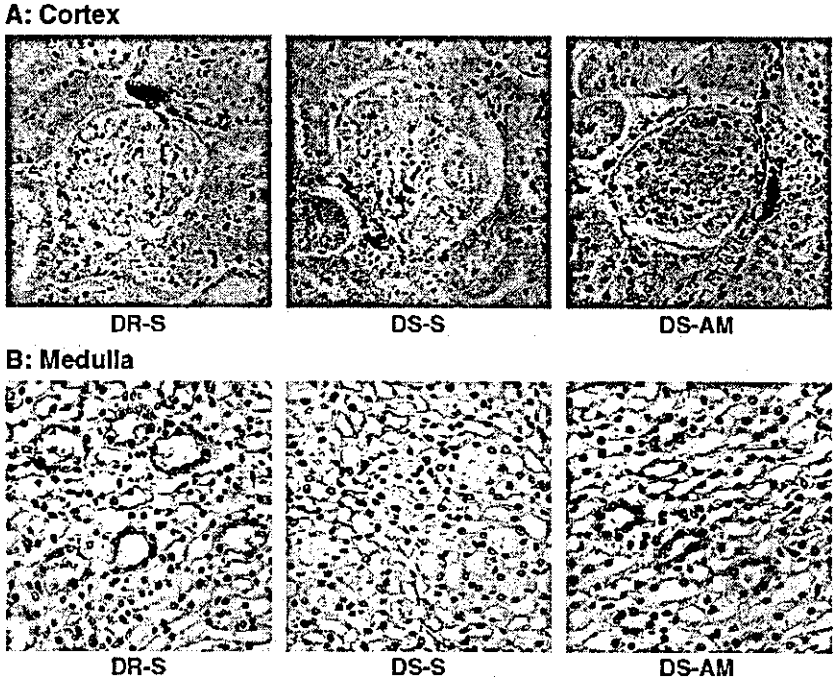

Fig. 3. Neuronal NOS immunoreactivity with a monoclonal antibody in the renal cortex and medulla at the end of the 4th-week in protocol 2.

in a reduction of urinary sodium excretion and an increase of blood pressure in DS rats. The expression of nNOS mRNA and immunoreactivity has been reported to exist in the macula densa and inner medullary collecting duct [19] in rats and renal nNOS specific activity was lower in DS rats than DR rats after a high sodium diet [5]. Interestingly, nNOS specific inhibition made the normally DR rats salt sensitive [20] and high sodium diet induced an increase in nNOS expression in the renal inner medulla of salt-resistant Sprague–Dawley rats [21]. Therefore, we evaluated the expression of nNOS. We observed a reduction in the nNOS level in the macula densa and inner medullary collecting duct in DS rats in the present Western blot and immunohistochemical analyses. Although we did not evaluate nNOS activity in the present study, our results suggested that one possible mechanism of salt-sensitive hypertension might be the reduced renal nNOS expression in the macula densa and inner medullary collecting duct in DS rats.

NO has been reported to be involved partly in vasodilation [22] and urinary sodium excretion [23] induced by adrenomedullin infusion. Recently, NO has been clarified to promote adrenomedullin gene expression in rat aortic vascular smooth muscle cells [24] and the maximal binding of adrenomedullin to its specific receptor in rat mesangial cells [25], suggesting that an accommodative interaction might exist between adrenomedullin and NO. Since we demonstrated that chronic adrenomedullin infusion attenuated salt-sensitive hypertension in association with the increased medullary eNOS expression and nNOS expression in the macula densa and inner medullary collecting duct, the attenuation of increasing of blood pressure by adrenomedullin infusion might be partly due to the increased eNOS and nNOS expression in the kidneys in DS rats.

In conclusion, our results suggest that chronic adrenomedullin infusion attenuates the increasing of blood pressure and decreases the degree of proteinuria probably in part through the increased renal medullary eNOS and nNOS expression in the macula densa and inner medullary collecting duct in DS rats and that renal adrenomedullin may serve as an endogenous protective mechanism against salt-sensitive hypertension. Our findings may open up the possibility of a new therapeutic strategy using adrenomedullin for salt-sensitive hypertension and renal injury.

Acknowledgements

Support for this study was provided in part by the Promotion of Fundamental Studies in Health Science of the Organization for Pharmaceutical Safety and Research (OPSR) of Japan, and by Grants-in-aid for Scientific Research (14571044) from Japan Society for the Promotion of the Science.

References

[1] Morimoto A, Uzu T, Fujii T, Nishimura M, Kuroda S, Nakamura S, et al. Sodium sensitivity and cardiovascular events in patients with essential hypertension. Lancet 1997;350:1734–7.
[2] Shultz PJ, Tolins JP. Adaptation to increased dietary salt intake in the rat. Role of endogenous nitric oxide. J Clin Invest 1993; 91:642–50.
[3] Baylis C, Harton P, Engels K. Endothelial derived relaxing factor controls renal hemodynamics in the normal rat kidney. J Am Soc Nephrol 1990;1:875–81.
[4] Tolins JP, Shultz PJ. Endogenous nitric oxide synthesis determines sensitivity to the pressor effect of salt. Kidney Int 1994; 46:230–6.
[5] Ikeda Y, Saito K, Kim JI, Yokohama M. Nitric oxide synthase isoform activities in kidney of Dahl salt-sensitive rats. Hypertension 1995;26:1030–4.
[6] Kitamura K, Kangawa K, Kawamoto M, Ichiki Y, Nakamura S, Matsuo H, et al. Adrenomedullin: a novel hypotensive peptide isolated from human pheochromocytoma. Biochem Biophys Res Commun 1993;192:553–60.
[7] Ichiki Y, Kitamura K, Kangawa K, Kawamoto M, Matsuo H, Eto T. Distribution and characterization of immunoreactive adrenomedullin in human tissue and plasma. FEBS Lett 1994;338:6–10.
[8] Jougasaki M, Wei C-M, Aarhus LL, Heublein DM, Sandberg SM, Burnett Jr JC. Renal localization and actions of adrenomedullin: a natriuretic peptide. Am J Physiol 1995;268:F657–63.
[9] Nishimatsu H, Suzuki E, Nagata D, Moriyama N, Satonaka H, Walsh K, et al. Adrenomedullin induces endothelium-dependent vasorelaxation via the phosphatidylinositol 3-kinase/Akt-dependent pathway in rat aorta. Circ Res 2001;89:63–70.
[10] Sakata J, Shimokubo T, Kitamura K, Nishizono M, Ichiki Y, Kangawa K, et al. Distribution and characterization of immunoreactive rat adrenomedullin in tissue and plasma. FEBS Lett 1994; 352:105–8.
[11] Gonick HC, Ding Y, Bondy SC, Ni Z, Vaziri ND. Lead-induced hypertension: interplay of nitric oxide and reactive oxygen species. Hypertension 1997;30:1487–92.
[12] Suga SI, Phillips MI, Ray PE, Raleigh JA, Vio CP, Kim YG, et al. Hypokalemia induces renal injury and alterations in vasoactive mediators that favor salt sensitivity. Am J Physiol Renal Physiol 2001;281:F620–9.
[13] Khan AI, Kato J, Kitamura K, Kangawa K, Eto T. Hypotensive effect of chronically infused adrenomedullin in conscious Wistar–Kyoto and spontaneously hypertensive rats. Clin Exp Pharmacol Physiol 1997;24:139–42.
[14] Lainchbury JG, Cooper GJ, Coy DH, Jiang NY, Lewis LK, Yandle TG, et al. Adrenomedullin: a hypotensive hormone in man. Clin Sci (Lond) 1997;92:467–72.
[15] Jougasaki M, Aarhus LL, Heublein DM, Sandberg SM, Burnett Jr JC. Role of prostaglandins and renal nerves in the renal actions of adrenomedullin. Am J Physiol 1997;272:F260–6.
[16] Kone BC, Baylis C. Biosynthesis and homeostatic roles of nitric oxide in the normal kidney. Am J Physiol 1997;272:F561–78.
[17] Kurtz A, Gotz KH, Hamann M, Sandner P. Mode of nitric oxide action on the renal vasculature. Acta Physiol Scand 2000;168:41–5.
[18] Ren YL, Garvin JL, Carretero OA. Role of macula densa nitric oxide and cGMP in the regulation of tubuloglomerular feedback. Kidney Int 2000;58:2053–60.
[19] Marsden PA, Hall AV, Brenner BM. Reactive nitrogen and oxygen intermediates and the kidney. In: Brenner BM, editor. The kidney, 5th ed. Philadelphia: WB Saunders; 1996. p. 719–21.
[20] Tan DY, Meng S, Manning Jr RD. Role of neuronal nitric oxide synthase in Dahl salt-sensitive hypertension. Hypertension 1999; 33:456–61.
[21] Mattson DL, Higgins DJ. Influence of dietary sodium intake on renal medullary nitric oxide synthase. Hypertension 1996;27:688–92.

[22] Hirata Y, Hayakawa H, Suzuki Y, Suzuki E, Ikenouchi H, Kohmoto O, et al. Mechanisms of adrenomedullin-induced vasodilation in the rat kidney. Hypertension 1995;25:790–5.
[23] Majid DS, Kadowitz PJ, Coy DH, Navar LG. Renal responses to intra-arterial administration of adrenomedullin in dogs. Am J Physiol 1996;270:F200–5.
[24] Hofbauer KH, Schoof E, Kurtz A, Sandner P. Inflammatory cytokines stimulate adrenomedullin expression through nitric oxide-dependent and-independent pathways. Hypertension 2002;39:161–7.
[25] Dotsch J, Schoof E, Schocklmann HO, Brune B, Knerr I, Repp R, et al. Nitric oxide increases adrenomedullin receptor function in rat mesangial cells. Kidney Int 2002;61:1707–13.

Journal of the American College of Cardiology
© 2005 by the American College of Cardiology Foundation
Published by Elsevier Inc.

Vol. 45, No. 4, 2005
ISSN 0735-1097/05/$30.00
doi:10.1016/j.jacc.2004.10.067

C-Type Natriuretic Peptide, a Novel Antifibrotic and Antihypertrophic Agent, Prevents Cardiac Remodeling After Myocardial Infarction

Takeshi Soeki, MD,* Ichiro Kishimoto, MD,* Hiroyuki Okumura, MD,* Takeshi Tokudome, MD,* Takeshi Horio, MD,† Kenji Mori, PHD,* Kenji Kangawa, PHD*

Suita, Osaka, Japan

OBJECTIVES We assessed the hypothesis that in vivo administration of C-type natriuretic peptide (CNP) might attenuate cardiac remodeling after myocardial infarction (MI) through its antifibrotic and antihypertrophic action.

BACKGROUND Recently, we have shown that CNP has more potent antifibrotic and antihypertrophic effects than atrial natriuretic peptide (ANP) in cultured cardiac fibroblasts and cardiomyocytes.

METHODS Experimental MI was induced by coronary ligation in male Sprague-Dawley rats; CNP at 0.1 μg/kg/min (n = 34) or vehicle (n = 35) was intravenously infused by osmotic mini-pump starting four days after MI. Sham-operated rats (n = 34) served as controls. After two weeks of infusion, the effects of CNP on cardiac remodeling were evaluated by echocardiograpic, hemodynamic, histopathologic, and gene analysis.

RESULTS C-type natriuretic peptide markedly attenuated the left ventricular (LV) enlargement caused by MI (LV end-diastolic dimension, sham: 6.7 ± 0.1 mm; MI+vehicle; 8.3 ± 0.1 mm; MI+CNP: 7.7 ± 0.1 mm, $p < 0.01$) without affecting arterial pressure. Moreover, there was a substantial decrease in LV end-diastolic pressure, and increases in dP/dt_{max}, dP/dt_{min}, and cardiac output in CNP-treated MI rats compared with vehicle-treated MI rats. Importantly, CNP infusion markedly attenuated an increase in morphometrical collagen volume fraction in the noninfarct region (sham: 3.1 ± 0.2%; MI+vehicle: 5.7 ± 0.5%; MI+CNP: 3.9 ± 0.3%, $p < 0.01$). In addition, CNP significantly reduced an increase in cross-sectional area of the cardiomyocytes. These effects of CNP were accompanied by suppression of MI-induced increases in collagen I, collagen III, ANP, and β-myosin heavy chain messenger ribonucleic acid levels in the noninfarct region.

CONCLUSIONS These data suggest that CNP may be useful as a novel antiremodeling agent. (J Am Coll Cardiol 2005;45:608–16) © 2005 by the American College of Cardiology Foundation

The mammalian natriuretic peptide system consists of three structurally homologous peptides, atrial natriuretic peptide (ANP), brain natriuretic peptide (BNP), and C-type natriuretic peptide (CNP) (1). The actions of the natriuretic peptides are modulated through membrane-bound receptors, two of which are guanylyl cyclase (GC)-coupled receptors (GC-A and GC-B). These receptors are linked to the cyclic guanosine monophosphate (cGMP)-dependent signaling cascade and mediate the biological actions of the peptides (2). Atrial natriuretic peptide and BNP are mainly released from the heart to act as circulating hormones, which bind to their specific receptor, GC-A, in the vascular tissue, kidney, and adrenal gland and induce vasodilation, natriuresis, and diuresis (3). C-type natriuretic peptide, which was originally isolated from porcine brain extracts (4), not only acts in the central nervous system, but also plays a role in the local regulation such as the suppression of neointimal formation after vascular injury (5) through its specific receptor, GC-B. Recently, we have shown that CNP was synthesized in cultured cardiac fibroblasts and that CNP inhibited both deoxyribonucleic acid (DNA) and collagen synthesis of cardiac fibroblasts more potently than ANP and BNP (6). C-type natriuretic peptide also has more potent antihypertrophic effects than ANP in cultured cardiomyocytes (7). These findings might be due to the relative abundance of GC-B over GC-A in cardiac fibroblasts and in cardiomyocytes (6,7). In addition, in a recent clinical study, CNP was produced by the hearts of patients with chronic heart failure, and its level in the coronary sinus correlated with mean pulmonary wedge pressure (8). These basic and clinical results suggest that CNP might represent an important local mediator in the heart.

Left ventricular (LV) remodeling after myocardial infarction (MI) is a major cause of subsequent heart failure and death (9). Postinfarction remodeling has been divided into an early phase (within 72 h), which involves expansion of the infarct zone, and a late phase (after 72 h), which is associated with time-dependent LV dilation, mural hypertrophy, and cardiac fibrosis (10). Given the inhibitory effects of CNP on cardiac fibrosis and hypertrophy in vitro, CNP might act against the progression of cardiac late remodeling after MI. Furthermore, because intravenously administered CNP has been demonstrated to have much less potent

From the *Department of Biochemistry, National Cardiovascular Center Research Institute, Suita, Osaka, Japan; and the †Department of Medicine, National Cardiovascular Center, Suita, Osaka, Japan. This work was supported, in part, by research grants from the Japanese Ministry of Education, Science, and Culture; the Japanese Ministry of Health, Labor and Welfare; the Program for Promotion of Fundamental Studies in Health Sciences of Pharmaceuticals and Medical Devices Agency; the Japan Cardiovascular Research Foundation; and the Kowa Life Science Foundation.

Manuscript received May 28, 2004; revised manuscript received October 22, 2004, accepted October 25, 2004.

Abbreviations and Acronyms

ANP = atrial natriuretic peptide
BNP = brain natriuretic peptide
CNP = C-type natriuretic peptide
cGMP = cyclic guanosine monophosphate
GC = guanylyl cyclase
LV = left ventricle/ventricular
MHC = myosin heavy chain
MI = myocardial infarction
PKG = cyclic guanosine monophosphate–dependent protein kinase
RV = right ventricle/ventricular
TGF = transforming growth factor

vasorelaxant and natriuretic activities than ANP (4,11), CNP is not expected to perturb systemic hemodynamics after massive MI while ANP or BNP is. However, there has been no in vivo evidence to directly prove these beneficial effects of CNP after MI. Therefore, in the present study, we have assessed the hypothesis that in vivo administration of CNP might attenuate cardiac late remodeling after MI. In addition, to elucidate the mechanism involved in the antifibrotic action of CNP, we investigated the action of cGMP/cGMP-dependent protein kinase (PKG) pathway on collagen synthesis by cardiac fibroblasts in vitro, and to clarify whether CNP is an important local mediator in the heart, we investigated the degree and source of endogenous CNP production in the infarcted heart.

METHODS

Model of MI. All experimental procedures were performed according to the guidelines for animal experimentation of National Cardiovascular Center. Male Sprague-Dawley rats (Nihon SLC, Hamamatsu, Japan) weighing 180 to 220 g were anesthetized with sodium pentobarbital (30 mg/kg, intraperitoneally). After left thoracotomy, the left coronary artery was ligated 2 to 3 mm from its origin using a 6-0 Prolene suture. The chest was closed, and the rats were allowed to recover. Sham-operated rats underwent the identical surgical procedure as described above without the actual coronary artery ligation.

Administration of CNP. Four days after coronary ligation, the rats with MI were randomly divided into two groups: one to be infused with synthetic CNP (MI+CNP, n = 36) and the other with vehicle (MI+vehicle, n = 42). The CNP group was then fitted with subcutaneous osmotic minipumps (model 2ML2, Alza Corp., Palo Alto, California) filled with synthetic CNP dissolved in a 5% glucose solution and set to release 0.1 μg/kg/min of the peptide for two weeks. The dose of CNP was chosen because our preliminary study revealed that CNP at this dose has no effects on arterial blood pressure and heart rate in rats. Glucose solution was infused in a similar manner in the control group. The pumps were connected to the left jugular vein by a polyethylene catheter. The synthetic CNP was kindly provided by Daiichi Suntory Pharma (Tokyo, Japan).

Noninvasive blood pressure and pulse rate. Systolic blood pressure and pulse rate were measured before MI and one day, one week, and two weeks after MI by the tail-cuff method without use of anesthesia (Softron, Tokyo, Japan).

Echocardiographic and hemodynamic studies. Echocardiographic studies were performed using an echocardiographic system equipped with a 15-MHz phased-array transducer (SONOS 5500, Hewlett Packard, Andover, Massachusetts) under anesthesia with sodium pentobarbital (30 mg/kg, intraperitoneally) 4 and 18 days after the experimental MI or sham operation as described previously (12). Rats with >20% fractional shortening or an early filling wave (E) velocity to atrial filling wave (A) velocity ratio of <3 in the echocardiographic study performed four days after MI were excluded from the study.

Eighteen days after the coronary ligation or sham operation, hemodynamic studies were performed under anesthesia as previously described (12). After completion of hemodynamic measurements, the hearts were arrested by the injection of 30 mM potassium chloride through the carotid artery, excised, and weighed.

Histological examination. After fixation, three cross-sections through the ventricles were obtained and embedded (n = 17 to 19 in each group). Paraffin sections (2 μm) were stained with Masson's trichrome for measurement of infarct size, hematoxylin and eosin for measurement of myocyte size, and Sirius red F3BA for determination of collagen volume fraction. The infarct size was expressed as previously described (13). For the measurement of cardiomyocyte cross-sectional area and diameter in the noninfarcted LV, a total of 30 myocytes sectioned transversely for area and longitudinally for diameter at the level of the nucleus were randomly chosen from each section at ×400 magnification, and traced. To measure collagen volume fraction, 16 fields in the border and remote myocardium of the noninfarcted LV and right ventricle (RV) walls per section were scanned at a magnification of ×200. The interstitial collagen volume fraction was measured while omitting fibrosis of the perivascular, epi-, and endocardial areas from the study. The collagen volume fraction was obtained by calculating the mean ratio of connective tissue to the total tissue area of all the measurements of the section. The collagen-positive areas from all sections were determined by a single investigator who was unaware of the experimental groups.

Northern blot analysis. Total ribonucleic acid (10 μg/lane) was extracted from the RV, noninfarcted LV, and infarcted LV (n = 10 in each group). Hybridization was carried out with cDNA probes for rat α-1 (type I) collagen, rat α-1 (type III) collagen, rat fibronectin, rat transforming growth factor (TGF)-β-1, rat ANP, and rat glyceraldehyde-3-phosphate dehydrogenase (GAPDH). We also used synthetic oligonucleotide probes for the α- and β-myosin heavy chain (MHC) messenger ribonucleic

JACC Vol. 45, No. 4, 2005
February 15, 2005:608–16

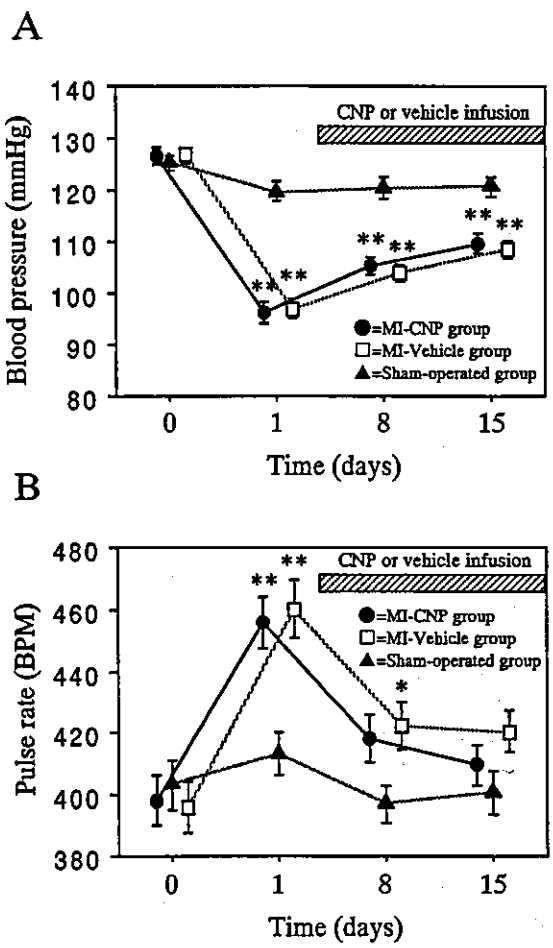

Figure 1. Time course of systolic blood pressure (A) and pulse rate (B) in sham-operated rats (**closed triangles**) and in rats with myocardial infarction (MI) before and during infusion of 0.1 μg/kg/min C-type natriuretic peptide (CNP) (**closed circles**) or vehicle (5% glucose solution) (**open squares**). Values are mean ± SEM. A p value for systolic blood pressure by two-way analysis of variance: group <0.001; time course <0.001; group/time course interaction <0.001, and a p value for pulse rate by two-way analysis of variance: group <0.05; time course <0.001; group/time course interaction <0.01. **p < 0.01, *p < 0.05 compared with the sham-operated group at same stage by Bonferroni multiple-comparison *t* test. BPM = beats/min.

acids (mRNA). The band intensity was estimated by a radioimage analyzer (BAS-5000, Fuji Film, Tokyo, Japan).

Collagen synthesis in vitro. Neonatal cardiac fibroblasts were prepared as described previously (14). The effects of CNP and a cGMP analog on collagen synthesis in cardiac fibroblasts were evaluated on subconfluent cultures by the incorporation of [^{3}H]proline into cells as previously described (6). In brief, after the preconditioning period, CNP with or without Rp-8-pCPT-cGMP (Calbiochem, San Diego, California), or 8-Bromo cGMP (Sigma, St. Louis, Missouri) was added, and 0.5 μCi of [^{3}H]proline was also added. After the cells were incubated for 24 h, the radioactivity of aliquots of the trichloroacetic acid-insoluble material was determined using a liquid scintillation counter.

Table 1. Echocardiographic Parameters

	Sham	MI+Vehicle	MI+CNP
4th day (before treatment)			
AWT diastole, mm	1.2 ± 0.01	1.0 ± 0.01*	1.0 ± 0.01*
PWT diastole, mm	1.3 ± 0.01	1.3 ± 0.01	1.3 ± 0.01
LVDd, mm	6.4 ± 0.1	7.0 ± 0.1*	7.0 ± 0.1*
FS, %	34 ± 1	16 ± 0.3*	15 ± 0.3*
E velocity, cm/s	89 ± 3	102 ± 2*	103 ± 3*
A velocity, cm/s	49 ± 2	18 ± 1*	19 ± 1*
E/A	1.9 ± 0.1	5.8 ± 0.2*	5.6 ± 0.1*
18th day (after treatment)			
AWT diastole, mm	1.2 ± 0.01	0.9 ± 0.02*	0.9 ± 0.01*
PWT diastole, mm	1.3 ± 0.01	1.5 ± 0.02*	1.4 ± 0.02*†
LVDd, mm	6.7 ± 0.1	8.3 ± 0.1*	7.7 ± 0.1*†
FS, %	35 ± 1	16 ± 0.4*	18 ± 0.4*†
E velocity, cm/s	88 ± 2	112 ± 3*	102 ± 3*‡
A velocity, cm/s	51 ± 2	19 ± 1*	26 ± 1*†
E/A	1.8 ± 0.05	6.2 ± 0.2*	4.2 ± 0.2*†

Values are mean ± SEM. *p < 0.01 compared with sham-operated group; †p < 0.01, ‡p < 0.05 compared with MI+vehicle group by analysis of variance and Bonferroni multiple-comparison t test.

A = atrial filling wave; AWT = anterior wall thickness; CNP = C-type natriuretic peptide; E = early filling wave; FS = fractional shortening; LVDd = left ventricular end-diastolic dimensions; MI = myocardial infarction; PWT = posterior wall thickness.

Quantitative reverse transcription-polymerase chain reaction. Endogenous mRNA expressions of ventricular CNP were evaluated in rats killed on day 3, 7, and 18 after MI (without CNP treatment) and on day 3 after sham operation (n = 6 in each group) with quantitative reverse transcription-polymerase chain reaction using a LightCycler system (Roche Applied Science, Penzberg, Germany) according to the manufacturer's instruction.

Immunohistochemical analysis. Immunohistochemical studies were performed to localize endogenous CNP in LV myocardium after MI. The section on day 7 after MI (in rats without CNP treatment) was stained with goat anti-CNP antibody (Santa Cruz Biotechnology, Santa Cruz, California) followed by Alexa-Fluor donkey anti-goat IgG antibody (Molecular Probes, Eugene, Oregon) and stained with rabbit fibronectin antibody (Sigma, St. Louis, Missouri) followed by tetrarhodamine isothiocyanate-conjugated goat anti-rabbit IgG antibody (DakoCytomation, Glostrup, Denmark).

Statistical analysis. All values are expressed as mean ± SEM. Differences among the groups were evaluated by one-way analysis of variance and two-way analysis of variance for repeated measurements, as appropriate. When a statistical difference was detected by analysis of variance, the Bonferroni method of adjusting for multiple pairwise comparisons was used. A value of $p < 0.05$ was considered statistically significant.

RESULTS

The effect of CNP on survival rate and infarct size. Among the MI rats, two of the CNP-infused rats and seven of the vehicle-infused rats died during the two-week infusion period. The survival rate of the MI+CNP group (94%) was higher than that of the MI+vehicle group (83%), but this

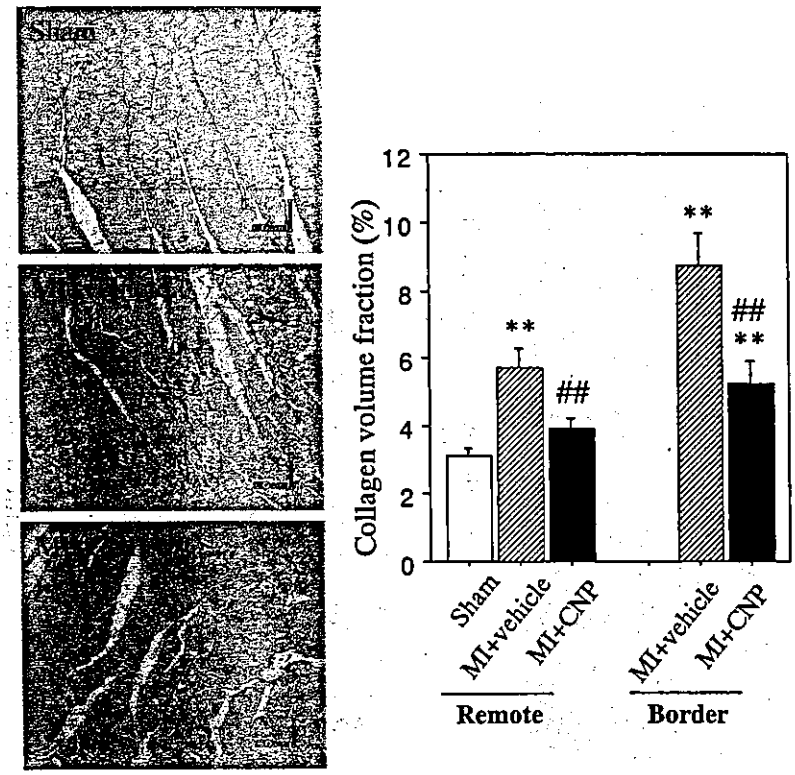

Figure 2. The effect of C-type natriuretic peptide (CNP) infusion on collagen volume fraction in the remote and border noninfarcted left ventricular area after myocardial infarction (MI). Representative photomicrographs of collagen volume stained with Sirius red in the remote noninfarcted LV (×200 magnification) **(left)** and quantitative morphometric analysis **(right)**. Values are mean ± SEM. **p < 0.01 compared with the sham-operated group; ##p < 0.01 compared with the MI+vehicle group by analysis of variance and Bonferroni multiple-comparison *t* test.

difference was not statistically significant by Kaplan-Meier survival analysis (p = 0.13). No rats died in the sham group. Therefore, the total numbers for final analysis were 34 rats in the MI+CNP group, 35 in the MI+vehicle group, and 34 in the sham group. There was no difference in infarct size between the MI+CNP and MI+vehicle groups (45 ± 1% and 46 ± 1%, respectively).

Serial change of noninvasive blood pressure and pulse rate. A significant reduction in the systolic blood pressure was observed in MI+CNP or MI+vehicle rats compared with the sham-operation rats during two weeks after the operation. As shown in Figure 1A, the systolic blood pressure was not perturbed by CNP infusion at any time points. The pulse rate in MI groups significantly increased at day 1 compared with sham animals and decreased gradually. The pulse rate was not significantly affected by CNP treatment at any time points (Fig. 1B).

The effect of CNP on echocardiographic and hemodynamic parameters. Table 1 shows echocardiographic assessments of cardiac geometry and function for the three groups of rats at the 4th and 18th days after MI. At the 4th day (before CNP infusion), when compared with sham, LV enlargement, decreased fractional shortening, and increased ratio of E to A velocities were seen in similar degree in both MI groups. At the 18th day (after two weeks of CNP infusion), hypertrophy of the posterior wall and the LV cavity enlargement caused by MI were significantly attenuated by CNP infusion, although thinning of the anterior wall was not changed; CNP also ameliorated the decrease of fractional shortening. Furthermore, CNP significantly improved LV diastolic filling pattern, resulting in a marked reduction in the ratio of E to A velocities (Table 1).

Table 2 also shows hemodynamic assessments for the three groups of rats at the 18th day after MI. No significant difference was noted in heart rate among the three groups. Mean arterial pressure and LV systolic pressure were lower

Table 2. Hemodynamic Parameters

	Sham	MI+Vehicle	MI+CNP
HR, beats/min	412 ± 5	421 ± 6	410 ± 5
MAP, mm Hg	120 ± 2	99 ± 2*	103 ± 2*
LVSP, mm Hg	139 ± 2	116 ± 2*	118 ± 2*
LVEDP, mm Hg	7 ± 0.4	18 ± 1*	13 ± 1*†
LV dP/dt_{max}, mm Hg/s	7,970 ± 156	5,019 ± 155*	5,743 ± 155*†
LV dP/dt_{min}, mm Hg/s	−6,216 ± 158	−3,791 ± 151*	−4,644 ± 147*†
CO, ml/min	98 ± 2	73 ± 2*	81 ± 2*†

Values are mean ± SEM. *p < 0.01 compared with sham-operated group; †p < 0.01 compared with MI+vehicle group by analysis of variance and Bonferroni multiple-comparison *t* test.

CNP = C-type natriuretic peptide; CO = cardiac output; HR = heart rate; LV dP/dt max or min = peak rate of left ventricular rise or fall; LVEDP = left ventricular end-diastolic pressure; LVSP = left ventricular systolic pressure; MAP = mean arterial pressure; MI = myocardial infarction.

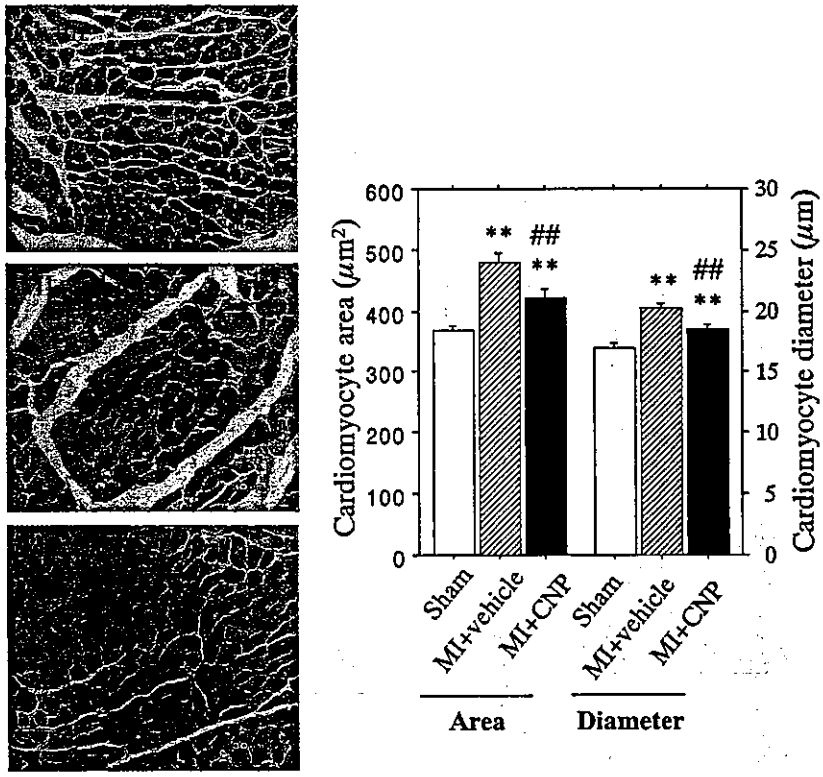

Figure 3. The effect of C-type natriuretic peptide (CNP) infusion on cardiac hypertrophy in the noninfarcted left ventricle. Representative photomicrographs of cardiomyocyte size stained with hematoxylin and eosin (×400 magnification) (**left**) and quantitative morphometric analysis of cardiomyocyte area and diameter (**right**). Values are mean ± SEM. **$p < 0.01$ compared with the sham-operated group; ##$p < 0.01$ compared with the myocardial infarction (MI) + vehicle group by analysis of variance and Bonferroni multiple-comparison *t* test.

in the MI+vehicle and MI+CNP groups than in sham, but there were no differences in these parameters between the two MI groups. Left ventricular end-diastolic pressure was higher, and the peak rate of contraction (dP/dt_{max}), the peak rate of relaxation (dP/dt_{min}), and the cardiac output were lower in MI+vehicle than in sham. As shown in Table 2, the MI-induced systolic and diastolic LV dysfunction was markedly improved by CNP.

The effect of CNP on cardiac collagen volume and hypertrophy. To clarify the mechanism of improved cardiac performance caused by CNP, we examined the effects of CNP treatment on collagen volume and mural hypertrophy in the noninfarcted region; CNP significantly ($p < 0.01$) attenuated an increase in morphometrical collagen volume fraction in the remote LV (Fig. 2) and RV (sham: 3.3 ± 0.3%; MI+vehicle: 5.5 ± 0.5%; MI+CNP: 4.2 ± 0.3%). Furthermore, CNP reduced an increase in collagen volume fraction more effectively in the border region of MI, in which fibrosis was more prominent compared with the remote zone (Fig. 2).

The cross-sectional area and diameter of myocytes in the noninfarcted LV significantly increased in MI+vehicle compared with sham, and hypertrophy of the myocytes was significantly ($p < 0.01$) inhibited by CNP infusion (Fig. 3). In agreement with the above results, the heart-weight-to-body-weight ratio, which was increased in the two MI groups compared with sham, was significantly ($p < 0.01$) lowered by CNP treatment (sham: 3.29 ± 0.03 g/kg; MI+vehicle: 3.96 ± 0.09 g/kg; MI+CNP: 3.69 ± 0.06 g/kg).

The effect of CNP on gene expression. To confirm the effects of CNP on cardiac remodeling, we examined the expression of several mRNAs associated with fibrosis and hypertrophy in the noninfarcted LV and RV after MI (Figs. 4A, representative autoradiograms, and 4B, quantitative analysis, n = 10 in each group). As shown in Figure 4, the increased mRNA expression of collagen type I and collagen type III after MI was significantly suppressed by treatment with CNP. The increased fibronectin mRNA expression tended to be decreased by CNP, but it was not significant. At the 18th day, mRNA expression of TGF-β-1, which is well known to be a fibrotic cytokine and to be upregulated in the acute phase of MI (15), was not different between MI rats with or without CNP infusion; CNP treatment resulted in suppression of the ANP mRNA level, which is a useful marker of cardiac fetal phenotype modulation after MI, and the β-/α-MHC ratio, which is a qualitative marker of cardiac hypertrophy, in the noninfarcted LV (Fig. 4). In the infarcted LV, mRNA levels of collagen type I, collagen type III, fibronectin, TGF-β-1, ANP, and β-/α-MHC were all increased in the MI+vehicle and MI+CNP groups compared with sham, but there was no difference in these